

LUND UNIVERSITY

Atmospheric chemistry and physics

Bachelor Thesis

Atmospheric decomposition of cyclic ethers

Ida Mexnell

2013-06-11

Supervisor: Elna Heimdal Nilsson

Examiner: Carl-Erik Magnusson



LUNDS
UNIVERSITET

Abstract

Renewable alternatives to fossil fuels are of importance nowadays since the use of fossil fuels is considered to stand for the largest contribution to global warming. In recent years, a group of cyclic ethers called furans have been proposed as potential renewable fuels. To enable evaluation of the usefulness of these compounds as fuels, it is important to understand their atmospheric chemistry since emission of fuel and its reaction products to the atmosphere is inevitable. The aim of this project is to investigate the environmental impact of the saturated compound tetrahydrofuran by determining its breakdown products and their approximate lifetimes. The study is made by analyzing experimental data for the photoreaction of tetrahydrofuran with the atmospheric oxidant Cl in a N₂/O₂ mixture and in pure N₂, respectively. The experimental data consist of sets of infrared spectra taken continuously during the reaction. Identification of products was made by comparing reference spectra of the products with the experimental spectra. Products identified in the N₂/O₂ experiment were butyrolactone, propyl formate, succinaldehyde, propionaldehyde, succinic anhydride, propionic acid, formic acid, hydrogen chloride, carbon monoxide and carbon dioxide. The product studies in the N₂ experiment were more speculative due to the absence of high-resolution reference spectra. However, it is likely that a major part of the products are chlorinated molecules. Further work is necessary to determine the complete product distribution and reaction mechanisms.

Table of contents

Abstract	i
Table of contents	ii
1. Background	1
1.1 Introduction	1
1.2 Biofuels	2
1.3 Aim of the project.....	2
1.4 Previous studies.....	2
2. Theory	4
2.1 Atmospheric lifetime	4
2.2 Molecules	4
2.3 IR-spectroscopy.....	6
2.4 Functional groups.....	8
3. Method	10
3.1 Experimental data.....	10
3.2 Analysis.....	11
4. Results and Discussion.....	16
4.1 N ₂ /O ₂ experiment.....	17
4.1.1 Primary products	17
4.1.2 Secondary products	20
4.1.3 Tertiary and later products.....	22
4.2 N ₂ experiment.....	25
5. Conclusion.....	34
References	35

1. Background

1.1 Introduction

Earth's climate has always been fluctuating but recent increase in the global temperature can most probably not be explained as a natural variability due to the short timescales. It is believed that the rapid proceeding of the global warming is an effect of human activities, in particular through the use of fossil fuels as one of our most important sources of energy.

Fossil fuel combustion is the primary cause of the increase in atmospheric carbon dioxide during the past century [1]. By replacing fossil fuels with renewable alternatives, the amount of carbon dioxide emitted into the atmosphere is generally considered to be reduced. Renewable fuels, such as biofuels produced from biomass, are renewable in the sense that the rate of production equals the rate of consumption and are therefore not expected to contribute to global warming. But not only is the global perspective of importance, especially if the fuels are to be used in vehicles. Also the environmental impact on the local air quality must be considered since the combustion process results in a series of reactions and will probably affect the local air composition. The investigation of the breakdown of the fuel includes studies in what products that form and their lifetime. Determination of the lifetimes can tell if they most likely affect the chemical composition close to the source or if they may reach the stratosphere and affect the stratospheric chemistry, which respond to a shorter and longer lifetime, respectively.

In recent years, furan compounds have been proposed as potential biofuels. Furans belong to a group of cyclic ethers with a five membered ring structure consisting of four carbon atoms and one oxygen atom. Figure 1 shows the unsaturated compound furan and the saturated compounds tetrahydrofuran (THF) and 2-methyl tetrahydrofuran (2-MTHF). This project will focus on THF and its role in atmospheric chemistry.

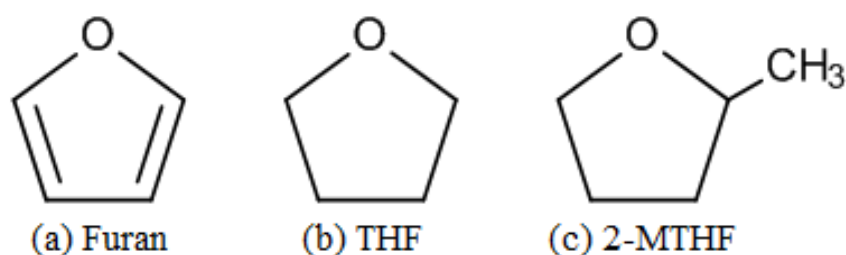


Figure 1. a) Unsaturated furan b) Saturated compound tetrahydrofuran c) Saturated compound 2-methyltetrahydrofuran.

1.2 Biofuels

In many ways, the use of fossil fuels is not sustainable, in particular due to their finite nature but also to the environmental impact on the global- as well on the local scale. These factors, among others, motivate the search for biofuels produced from biomass. Since the transportation sector is one of the main energy consumers, liquid biofuels are believed to play a large role in the future as a substitute to fossil fuels used in vehicles, such as gasoline and diesel. Two liquid biofuels used widely today are ethanol (C_2H_5OH) and biodiesel, produced from sugars and vegetable oil respectively [2].

Both are in the category first generation biofuels, defined as those produced from food-based crops, such as sugar cane, maize and corn, using conventional technology [3]. Although these fuels show indications to reduce the greenhouse gas emissions they are associated with several disadvantages. The production competes with food production and an increased use of first generation biofuels may lead to escalated food prices and problems with the food supply. Furthermore, an increased demand for agricultural crops may lead to larger problems associated with agriculture such as deforestation, fertilizers and negative impact on the biodiversity [3].

Many of the problems related to the first generation biofuels are believed to be avoided using later generation biofuels produced from non-edible feedstock using more advanced technology. At present, there are both technical and economic challenges to overcome before these fuels can come into commercial use but they have potential to be economically favourable in the long term [3].

Concerning the environmental impact on the local scale, studies have been made that show a change in atmospheric composition if the fossil fuels were replaced by biofuels. Especially a study is made showing increased levels of harmful tropospheric ozone for the widely used biofuel ethanol compared to the fossil fuel case [4]. The formation of ozone can be explained by a significant increase of formaldehyde and acetaldehyde, two important ozone precursors, which also was shown in the study [4]. Hence, research on biofuel emissions is important for prediction of future environmental issues.

1.3 Aim of the project

Use experimental results to determine the product distribution from the reaction of THF with Cl in the presence and absence of O_2 .

1.4 Previous studies

Rate coefficients for THF, obtained with the relative rate method, have been investigated in several studies, both in reaction with OH [5] and in reaction with Cl [6, 7]. The results from the Cl-initiated reaction show a small difference but are in agreement within the reported experimental uncertainty. THF shows a high reactivity towards both oxidizers, but the rate coefficients for reaction with Cl are up to two orders of magnitude larger than for reaction with OH, which is analogous for the majority of organic compounds [8]. The studies are in agreement that OH is the major oxidizer of THF worldwide but in the marine boundary layer and polluted industrial and urban areas where the Cl concentration can reach high values it will contribute significantly to the degradation of THF.

No product distribution from either the OH-radical or the Cl-atom initiated degradation of THF has been investigated experimentally, only a theoretical study has been presented this far [9]. The theoretical study presents a couple of possible reaction paths with kinetic differences. However, irrespective of the followed path, all final products are the same. Experimental studies of the product distribution have been made for unsaturated furan, both the OH-initiated- [10] and Cl-initiated [11] degradation. In the OH-initiated reaction, butenedial ($C_4H_4O_2$) is formed as a major primary product and glyoxal ($C_2H_2O_2$), formic acid (HCOOH) and carbon dioxide (CO_2) as secondary products. The Cl-initiated degradation study presents several chlorine-containing products in the major reaction pathway.

2. Theory

2.1 Atmospheric lifetime

The atmospheric lifetime of a chemical species is a measure of how long the species will reside in the atmosphere before it is removed. By calculating the lifetime one can estimate the distribution of the species since the lifetime is related to atmospheric mixing times. Mixing times have strong directional- and layer dependences. Vertical mixing in the troposphere takes about one week, whereas horizontal mixing takes about a year. Mixing between different atmospheric layers, e. g. the troposphere and the stratosphere takes even longer due to the temperature inversion in the stratosphere, hence only long lived species can be transported to the stratosphere.

One of the most important removal processes in the troposphere is reaction with the hydroxyl radical (OH) and OH is generally considered to be the main oxidant for hydrocarbons. The concentration of OH is relatively high around the world but shows local variations depending on the presence of reactants [1]. For example, the concentration is in general higher on the southern hemisphere than on the northern due to the higher amount of anthropogenic emissions on the northern hemisphere, with which the OH radical reacts. The local variation is also dependent on the production, due to the high reactivity and relatively short lifetime of OH. It is produced by photolysis of ozone and further reaction with H₂O, favouring the production in the tropics where the incoming solar radiation and humidity are high [12].

Another important oxidant, especially in marine regions, is the chlorine atom. Chlorine is often in the form of NaCl, derived from sea-salt and must undergo a couple of reactions to be available in the gas-phase chemistry. Chlorine oxidation may also play an important role in polluted industrial areas, since the Cl atom is released by photolysis of several Cl-containing substances derived from anthropogenic emissions [8]. The oxidation process of the Cl atom is similar to OH but it shows a higher reactivity, with rate coefficients that are an order of magnitude or more. Hence, the Cl atom contributes significantly to tropospheric oxidation [13].

The Cl atom might be even more powerful in the stratospheric chemistry since many chlorine-containing compounds, both from anthropogenic and natural sources, primarily degrade by high energetic photodissociation, and thus have a sufficiently long lifetime to reach the stratosphere. In the stratosphere, the Cl atom is highly reactive towards ozone and initiates an effective destruction cycle [12].

2.2 Molecules

If nothing else is stated, the following section is obtained from *Quantum Chemistry and Spectroscopy* by Tomas Engel (2013) [14].

Molecules are a certain number of atoms held together by chemical bonds. A chemical bond is formed if the energy of the molecule is lower at an equilibrium distance, R_e between the atoms than the energy of the atoms separately, see Figure 2.

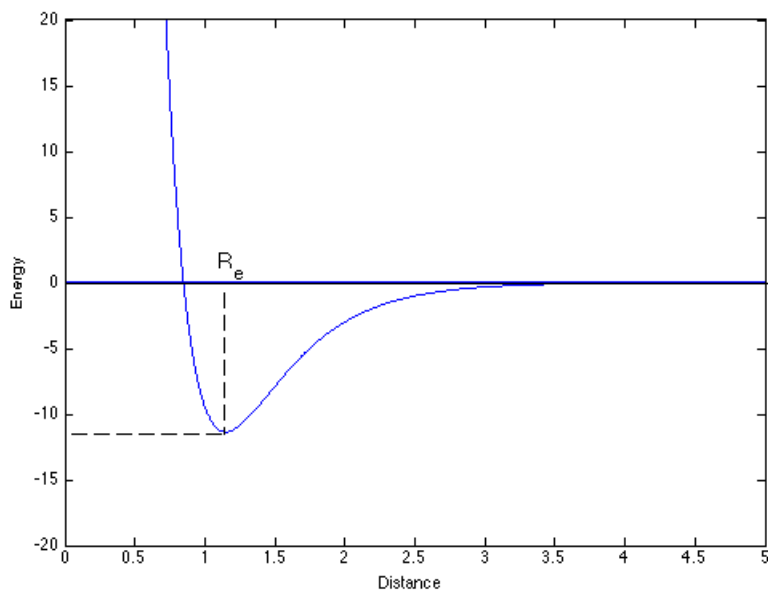


Figure 2. Molecular potential energy curve for a diatomic molecule.

The molecular potential energy curve shown in Figure 2 is obtained using the Born-Oppenheimer approximation, in which it is assumed that the nucleus, which is much heavier than the electron, will move with negligible speed relative the electron. Thus the nuclei may be treated as stationary and the Schrödinger equation can be solved for the electrons at different internuclear distances in a diatomic molecule. Close to the minimum of the potential is the bond dissociation energy, which is simply the energy needed to dissociate the molecule into free atoms.

A molecule has translational, vibrational and rotational motions, which all of them contribute to the total energy of the molecule. Each of the motions is described by quantum mechanical operators and thus has its own energy spectrum and energy eigenvalues.

The vibrational motion is based on the harmonic oscillator and the vibration can be thought of as an oscillation around the equilibrium bond length of the molecule. However, harmonic oscillations are given by a parabolic function, which is a good approximation only at the bottom of the real molecule potential energy curve in Figure 2. In order to reproduce the shape of the real potential more closely one uses the Morse potential, a mathematical function for which the corresponding Schrödinger equation can be solved analytically. The energy scale of the vibrations is much smaller than the electronic excitation energies and the vibrational states can be seen as the fine structure of each electronic state. The rotational motion is, to a large extent, well described by the rigid rotor model. The molecule is assumed to be rotating around its central axis with a fixed bond length. The energy scale of the rotations is much smaller than the vibrational energies and the rotational states can be seen as the fine structure of each vibrational state.

Since the energy levels are quantized, transitions can be made between different levels if certain selection rules are satisfied. Transitions are often made during absorption or emission of a photon, whose energy corresponds to the energy difference between the two levels.

Electronic transitions correspond to energies in the ultraviolet or visible region of the electromagnetic spectrum ($1 \cdot 10^{-8}$ - $4 \cdot 10^{-7}$ resp. $4 \cdot 10^{-7}$ - $7 \cdot 10^{-7}$ m), vibrational transitions to energies in the infrared region ($7 \cdot 10^{-7}$ - $1 \cdot 10^{-3}$ m) and pure rotational transitions to the microwave region (0.001-0.1 m).

2.3 IR-spectroscopy

If nothing else is stated, the following section is obtained from *Quantum Chemistry and Spectroscopy* by Tomas Engel (2013) [14].

Spectroscopy is a powerful tool for investigations on molecular level and the technique is based on the light-matter interaction, namely the molecular transitions that occur between allowed energy states in the interaction with electromagnetic radiation. As mentioned in the previous section, the energy of molecular vibrations corresponds to the infrared region of the electromagnetic spectrum, thus a common method to detect and measure these vibrations is infrared absorption spectroscopy.

In general, the infrared spectrum of a sample is obtained by passing a beam of light through a cell where the sample is confined, followed by detection of the transmitted light. The relationship between the intensities of the incident and transmitted IR light, the molar concentration of the sample and the absorption path length is given by Beer-Lamberts law.

$$I = I_0 e^{-\varepsilon(\lambda)Nl}$$

I and I_0 are the transmitted and incident light intensity, respectively, $\varepsilon(\lambda)$ is the molar absorption coefficient, N is the molar concentration of the sample and l is the path length. From Beer-Lamberts law, expressions can be derived for the transmittance, T and absorbance, A .

$$T = \frac{I}{I_0}$$

$$A = \ln\left(\frac{I_0}{I}\right)$$

A technique to obtain infrared spectra has been developed called Fourier Transform Infrared Spectroscopy (FTIR). The principle for FTIR is that the light is split into two beams, one is sent through the sample towards a fixed mirror at the end of the cell and the other is sent towards a movable mirror. The reflected beams are recombined and sent to the detector. Due to the movable mirror it is possible to determine which frequencies that have been absorbed by the sample since the recombined waves give rise to an interference pattern, called an interferogram. The interferogram is converted to a spectrum using Fourier transform techniques and the spectrum is usually obtained by plotting transmittance or absorbance versus wavenumber. The advantage using FTIR compared to the conventional method is primarily the possibility to measure over the whole range of frequencies simultaneously thus the spectra can be obtained much quicker.

Not every molecule can be seen in an IR-spectrum, i.e. is IR-active. The absorption of the infrared radiation requires that the molecular vibration causes a change in the dipole moment

of the molecule. The result is that centrosymmetric molecules such as N_2 , O_2 and Cl_2 will not be IR-active but HCl , CO and CO_2 will.

The IR-spectrum for CO is shown in Figure 3. Smaller molecules, such as CO , show a more detailed structure than larger molecules which often have a large number of vibrations affecting each other. The characteristic pattern shown in Figure 3 is not only the vibrational transition but also the change in rotational motion due to the vibrational change. A schematic picture of the allowed transitions is shown in Figure 4. Vibrational- and rotational states are denoted n and J , respectively. The region with $\Delta J=+1$ transitions is called the R-branch and the region with $\Delta J=-1$ transitions is called the P-branch, corresponding to higher and lower frequencies, respectively. Thus, in Figure 3 the R-branch is seen to the left in the spectrum and the P-branch to the right.

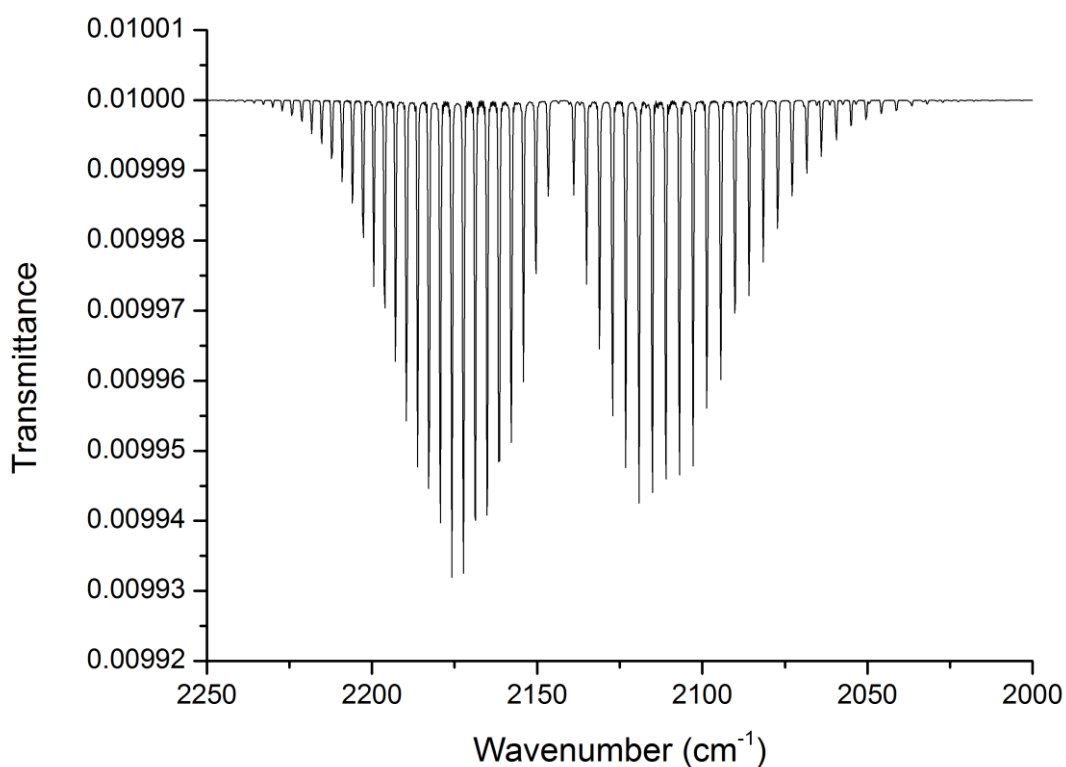


Figure 3. IR-spectrum of CO [22].

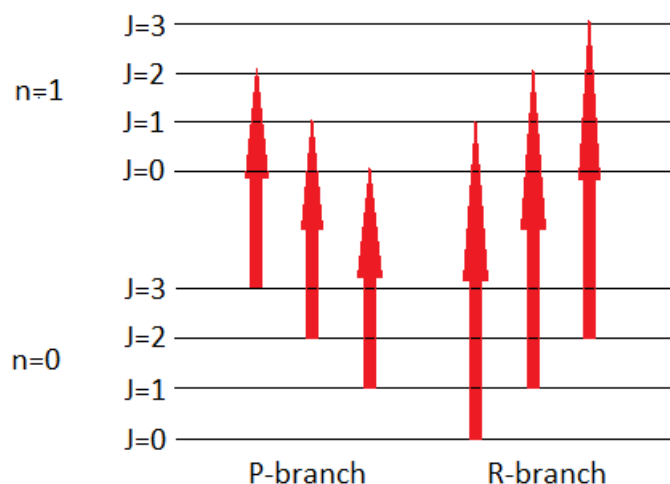


Figure 4. Allowed transitions between different energy levels in a molecule with n as the vibrational state and J as the rotational state.

2.4 Functional groups

If nothing else is stated, the following section is obtained from *Spectroscopic methods in organic chemistry* by Dudley H. Williams and Ian Fleming (1995) [15].

Useful when determining the structure of a molecule using IR-spectroscopy is the presence of functional group frequencies. It is vibrations of individual bonds or functional groups that give rise to absorption in a relatively narrow frequency range. The vibrations can be of different character, namely stretching, bending, rocking, twisting or wagging, see Figure 5. These types of vibrations will be found in different frequency ranges even if they correspond to the same functional group. The characteristic group frequencies are primarily seen in the region above 1500 cm^{-1} but some are present also below 1500 cm^{-1} , in a region called the fingerprint region; fingerprint in the sense that it is primarily the combined vibrations of larger molecules, which are characteristic for that specific molecule that will be found there.

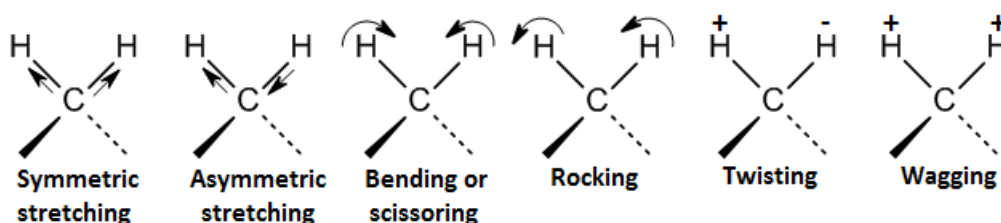


Figure 5. Vibrational types for the methylene group.

There are some general features that can be pointed out when it comes to vibrational frequencies. Absorbing frequencies corresponding to stretching vibrations are in general higher the greater the strength is between two similar atoms, i.e. triple bonds vibrate at higher frequency than double bonds and double bonds at higher frequency than single bonds. This is also true for larger molecules e.g. unsaturated hydrocarbon chains, which means that are double bonds in the molecule, absorbing in a different region than the saturated counterparts,

which have only single bonds. The vibration frequency also depends on the weight of the atoms. For example, stretching vibrations for single bonds to hydrogen give rise to absorption at high frequencies as a result of its low mass. A couple of functional groups and their characteristic frequencies at which they absorb are shown in Table 1.

Table 1. Absorption ranges for functional groups [15].

Functional group	Name and vibrational type	Absorption range
C—H	C-H stretch C-H deformation	3050-2850 cm ⁻¹ 1470-1430 cm ⁻¹
$\begin{array}{c} \text{H} \\ \\ \text{C}-\text{H} \\ \\ \text{H} \end{array}$	CH ₃ deformation	1390-1370 cm ⁻¹ 1470-1430 cm ⁻¹
O—H	O-H bending	1410-1260 cm ⁻¹
C—O	C-O stretch	1300-1040 cm ⁻¹
C=O	Carbonyl stretch	1850-1700 cm ⁻¹
$\begin{array}{c} \text{H} \\ \\ \text{C}-\text{O} \end{array}$	Alcohols	1150-1040 cm ⁻¹ 1410-1260 cm ⁻¹
$\begin{array}{c} \text{O} \\ \\ \text{C} \\ \\ \text{O}-\text{H} \end{array}$	Saturated carboxylic acids	3000-2500 cm ⁻¹ 1725-1700 cm ⁻¹
$\begin{array}{c} \text{O} \\ \\ \text{C} \\ \\ \text{Cl} \end{array}$	Saturated acid chlorides	1815-1790 cm ⁻¹
$\begin{array}{c} \text{O} \\ \\ \text{C} \\ \\ \text{H} \end{array}$	Saturated aldehydes	1740-1720 cm ⁻¹
C—O—C	Saturated ethers	1150-1070 cm ⁻¹
$\begin{array}{c} \text{O} \\ \\ \text{C}-\text{O} \end{array}$	Saturated esters	1750-1735 cm ⁻¹ 1300-1050 cm ⁻¹

3. Method

3.1 Experimental data

In this project, the reaction between THF and Cl was investigated in two different environments, a N₂/O₂ mixture respectively in pure N₂. The N₂/O₂ mixture was of air composition i.e. 79 % N₂ and 21 % O₂. Even though the use of OH as a reactant would be slightly more interesting in an atmospheric point of view, Cl is preferable since it reacts in a similar way but gives cleaner spectra. The production of OH needs both O₃ and H₂O which gives a lot of undesirable noise and complicates the product analysis. Reactions in both N₂/O₂ and N₂ are performed in order to determine the role of O₂ in the reaction mechanism. Since there are fewer reactants in the N₂ experiment, the product analysis is believed to be simpler.

The experimental work was not a part of this project and data was obtained from the Bachelor Thesis report *Furans – The potential atmospheric impact of a next-generation bio fuel* by Stina Ausmeel (2012) [16]. The experiments were performed in a photochemical reactor at Copenhagen Center for Atmospheric Research in 2012 [17]. They were made under atmospheric conditions at a temperature of 25 °C and a pressure of 980 mbar. In each environment, two experiments were made with different initial concentrations in order to ensure that all products were registered since their peaks have varying strength, see Table 2. However, in both cases the partial pressure of initiated chlorine was ten times higher than of THF. An excess of chlorine is desirable to avoid other reactions to take place than with the Cl atoms. An UV-lamp emitting light in the wavelength range 325-380 nm was used in order to dissociate Cl₂ into reactive Cl atoms, required for the reaction to take place. The photolysis was made in series of 10 photolysis intervals. The first intervals were approximately 1 second and then successively increased from 2 seconds up to 10 seconds. These short intervals are needed due to the high reactivity of THF and it is desirable if the reaction does not take place at once but in several steps. After each photolysis interval, a pause of 2 minutes was made before the spectrum was taken to allow the initiated chemistry to fully proceed. The spectra have the resolution 0.5 cm⁻¹ and were performed with 32 scans. The spectral interval is in the mid-IR range from about 950 cm⁻¹ to 3200 cm⁻¹.

Table 2. Experimental data [16].

Initial compounds	Partial pressures [10 ⁻³ mbar]	Total pressure [mbar]
THF Cl ₂ N ₂ /O ₂	4.3 150.8	985
THF Cl ₂ N ₂ /O ₂	9.9 169.7	980
THF Cl ₂ N ₂	4.6 159.8	983
THF Cl ₂ N ₂	9.6 242.2	978

3.2 Analysis

In the product analysis, the degradation mechanism and product distribution for THF in N_2/O_2 and N_2 are determined. The product formation can be visualized in the photolysis series with the computer program OPUS. In OPUS it is possible to subtract reference spectra for known products to enhance the visualization of unknown products. Figure 6 shows spectra from the N_2/O_2 and N_2 experiment. The initial spectra show only the reactants while the last spectra show only products. The intermediate steps show the formation and growth of products.

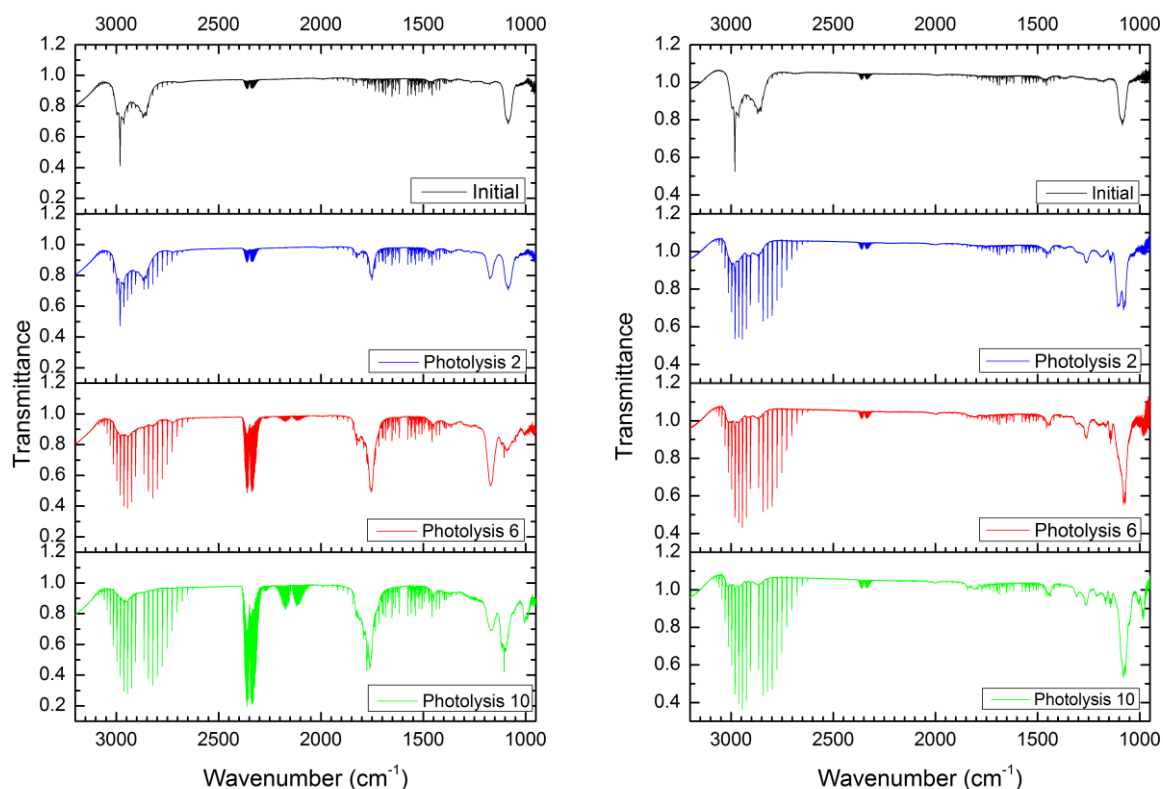


Figure 6. Spectra in the series for; Left: N_2/O_2 experiment Right: N_2 experiment. Note the scale difference on the y axis for the left and the right spectra.

By identification of functional groups one can get information of the molecular structure. A certain molecule usually has many absorption frequencies, which further on are denoted peaks. Since many products are formed in a reaction, it is difficult to know which peaks that belong to which molecule. Some peaks may overlap which further complicates the identification. To group the peaks one can study their growth rate. Figure 7 shows spectra from the experiment with N_2 . To a first approximation, the 1143 cm^{-1} peak can be grouped with the 1260 cm^{-1} peak since both grow until photolysis 6 and then start to decrease. Also, peak 1165 cm^{-1} can be grouped with the 1210 cm^{-1} peak since they have a similar growth rate.

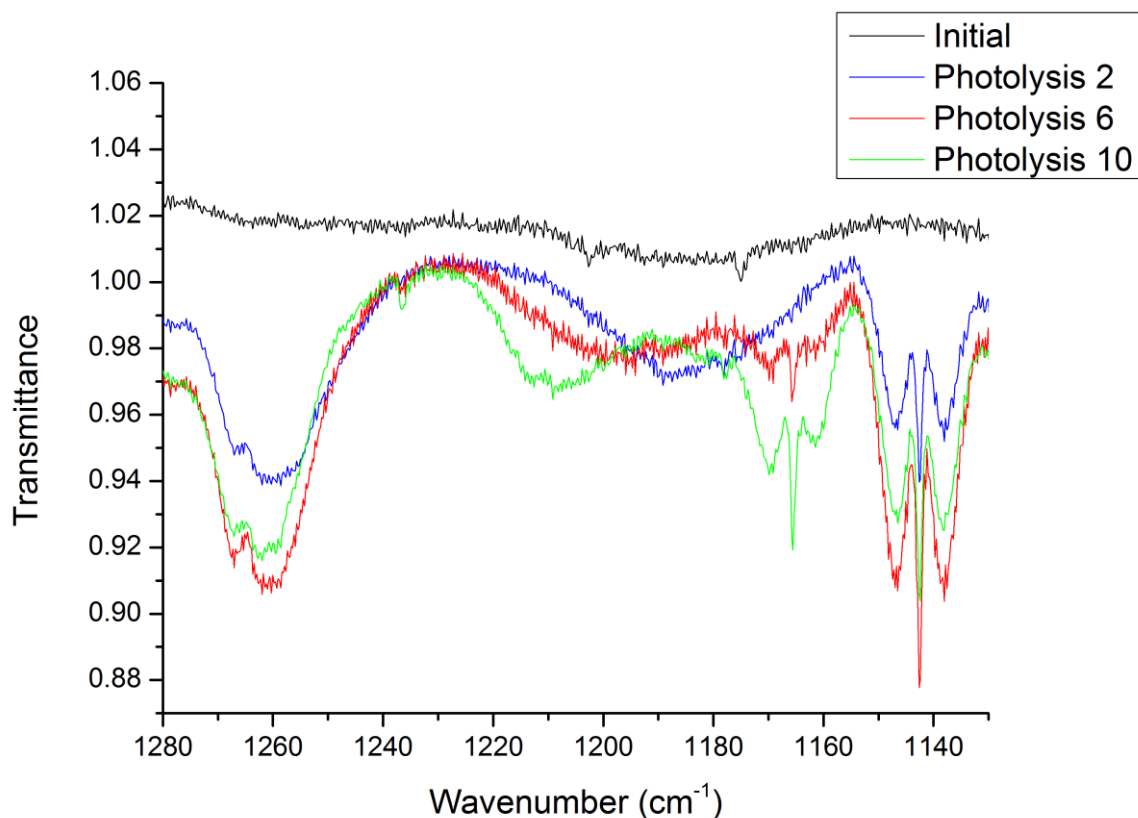


Figure 7. The fingerprint region for N_2 experiment.

The procedure described above may result in qualified guesses of products and several methods are used in order to verify them. The experimental spectra can be compared with existing spectra obtained from NIST [18] and the EUROCHAMP database [19]. The resolution of these spectra is varying but can in most cases be used for verification. The undetermined products, to which no spectra were found in the databases, were computed with the computer program Gaussian 09 [20]. The calculated spectra give only the major features of the structure, see Figure 8.

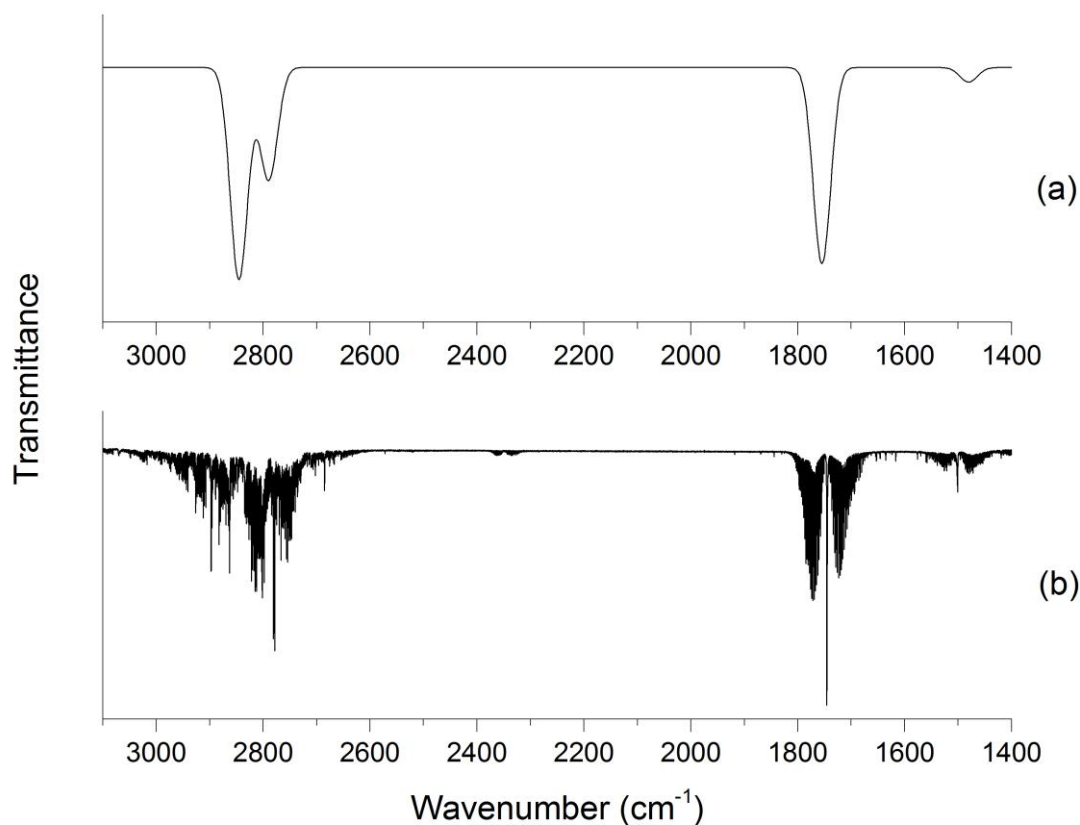


Figure 8. Spectra of H_2CO a) Calculated with Gaussian 09 [20] b) Experimental.

When a product is known, its change of concentration with photolysis time can be obtained using MALT (Multi-Atmospheric Layer Transmission), a program for simulation and fitting of infrared spectra [21]. The program takes a chosen region of the experimental spectrum as input. With a spectral fitting procedure that takes several parameters, such as pressure broadening and temperature into account a synthetic spectrum is obtained. The simulation of the spectrum is made using either line parameters from the HITRAN database [22], or high-resolution reference spectra. The output is the experimental spectrum, the synthetic spectrum and the residual, which is simply the difference between the first two. Figure 9 shows the fitting of CO in the N_2/O_2 experiment. Since the concentration of the substance is known in the reference spectrum, the concentration in the experimental spectrum is obtained from the program after the fitting procedure. The program is also able to distinguish overlapping peaks from components of a gas mixture. Figure 10 shows the reference spectra for THF and HCl used in the fitting procedure and Figure 11 shows the output components.

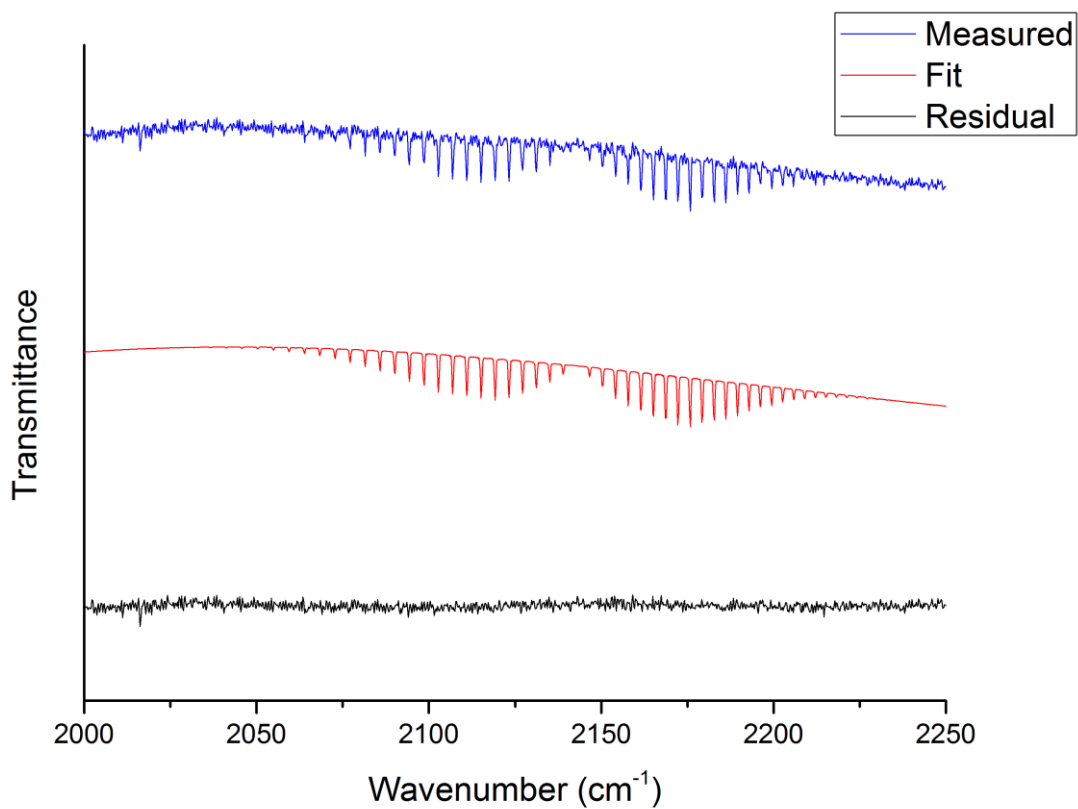


Figure 9. MALT components for the fitting of CO in N_2/O_2 experiment photolysis 5 [22]. The spectra are offset vertically.

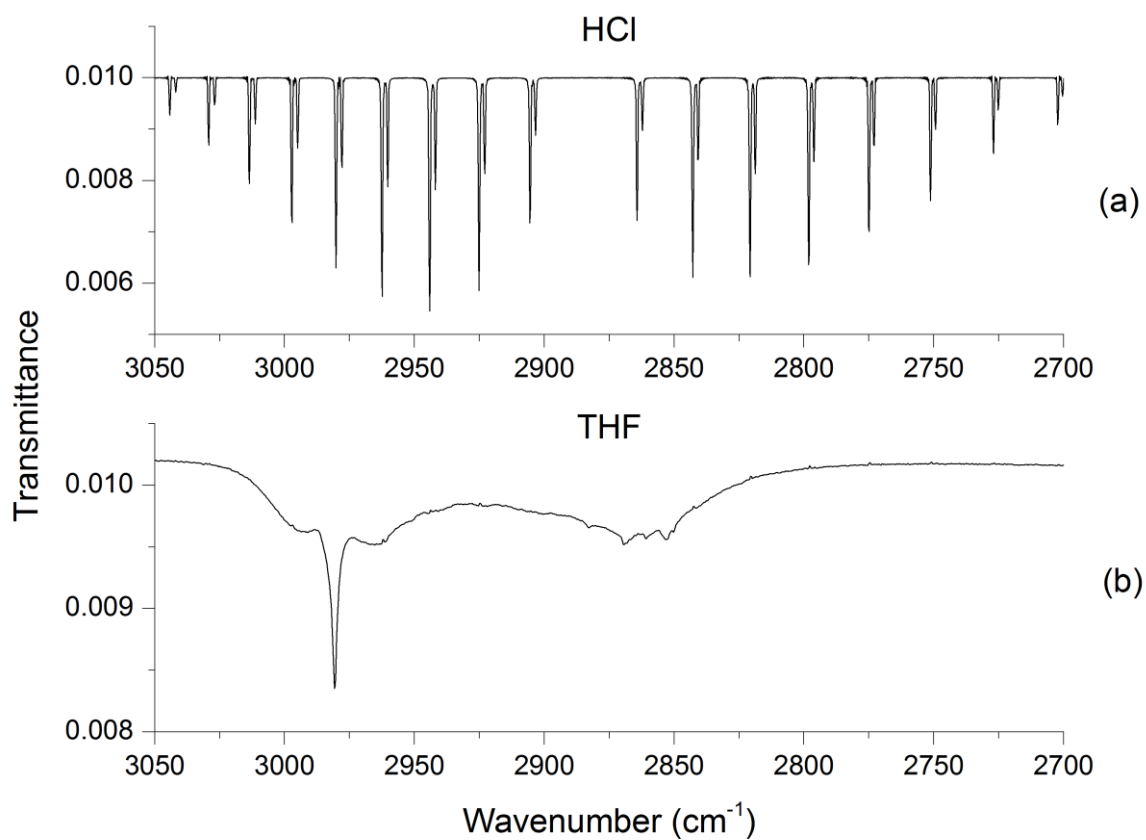


Figure 10. Reference spectra for a) HCl [22] and b) THF used in the fitting procedure.

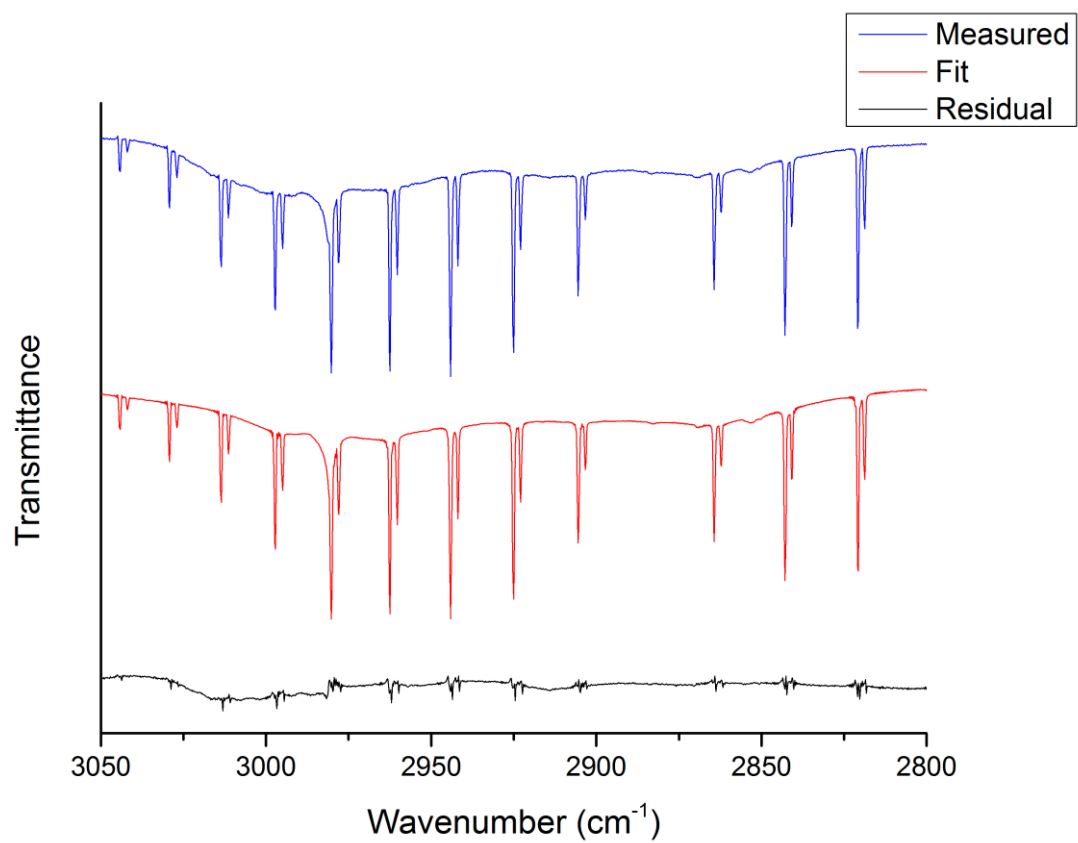


Figure 11. MALT components for the fitting of THF and HCl in N₂ experiment photolysis 4. The spectra are offset vertically.

4. Results and Discussion

The results of product studies of the Cl-atom initiated oxidation of THF are presented in this section, both in N_2/O_2 mixture and in N_2 . Initially, a general picture of the product distribution for both environments is obtained by a rough analysis of Figure 6. Similarities in the two spectra are the approximate same amount of HCl building up during the experiments and the continuous decrease of absorption in the 3000 cm^{-1} region. In the intermediate region of the spectra, N_2/O_2 shows a continuous increase of CO and CO_2 , which peaks are identified at 2150 cm^{-1} and 2350 cm^{-1} , respectively, while N_2 shows a very small amount of CO and CO_2 building up. A close inspection of the region showing the CO and CO_2 is shown in Figure 12. N_2/O_2 shows strong absorption in the carbonyl region ($1850\text{--}1700\text{ cm}^{-1}$) while there are only indications of absorption in the same region of the N_2 spectra. Both environments show activity in the fingerprint region but there are fewer peaks in the N_2/O_2 spectra than in the N_2 spectra. None of the spectra shows peaks in the $1700\text{--}1500\text{ cm}^{-1}$ region which indicates an absence of alkenes, unsaturated compounds containing at least one carbon-carbon double bond, which usually show absorption in that region [15]. Note that ethylene (C_2H_4), which is the simplest alkene, does not absorb in that region due to the symmetry of that molecule.

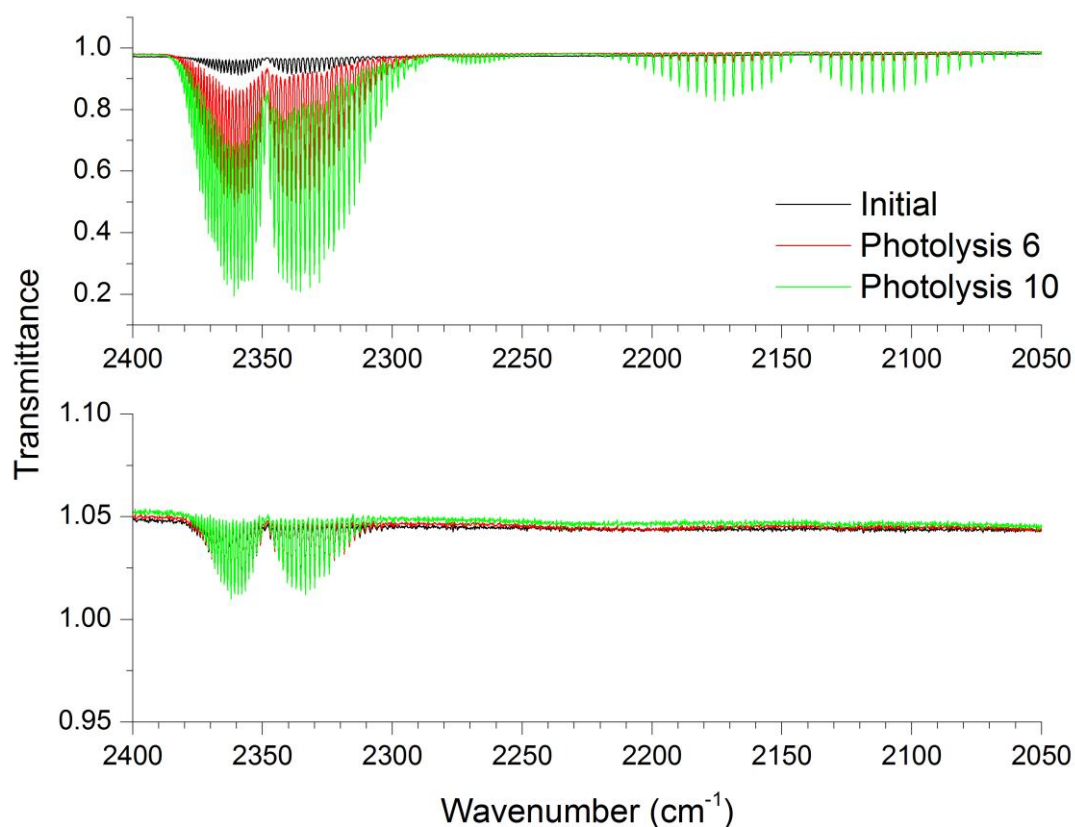
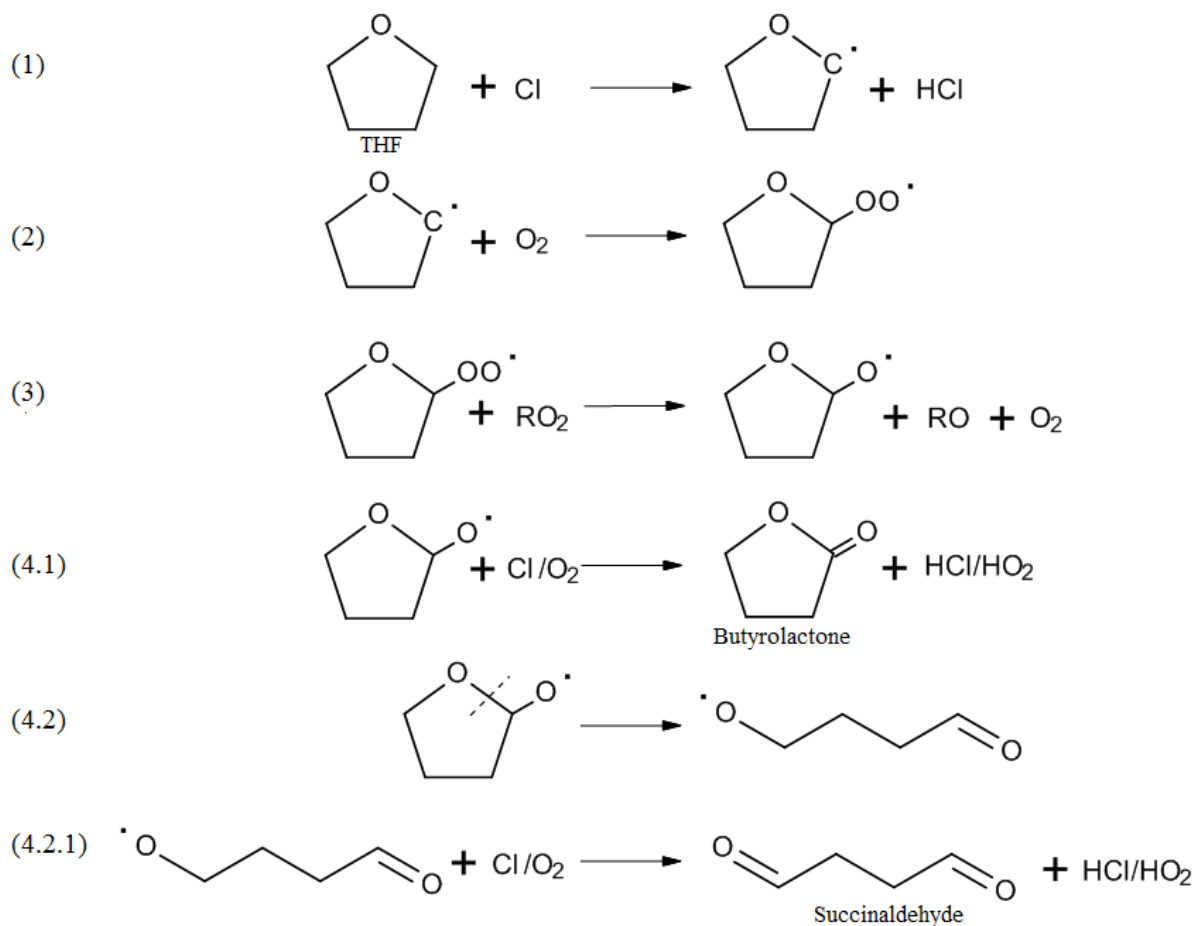


Figure 12. The region showing the absorption of CO_2 at 2350 cm^{-1} and CO at 2150 cm^{-1} in N_2/O_2 (upper panel) and in N_2 (lower panel). Note the scale difference on the y axes.

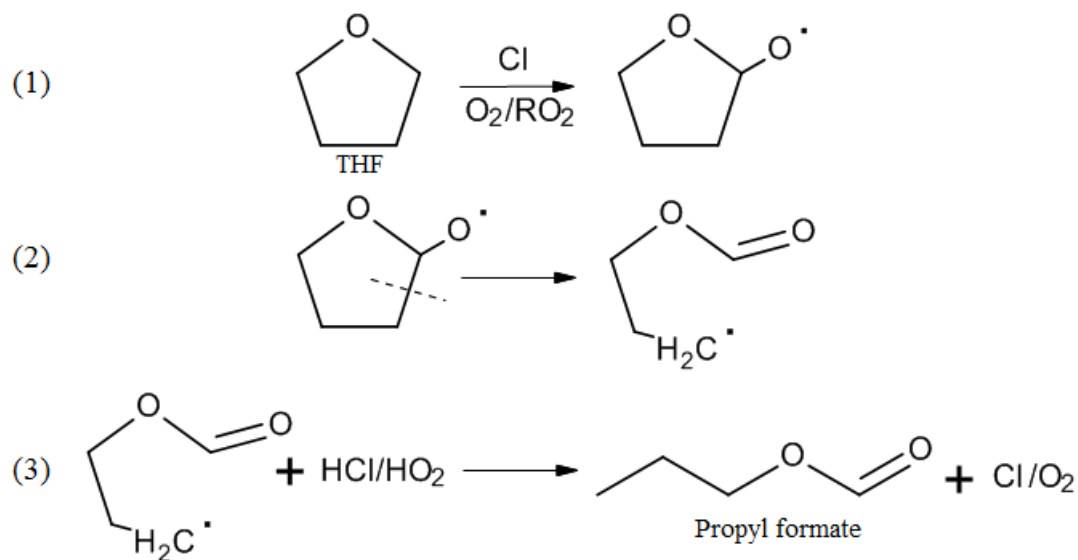
4.1 N₂/O₂ experiment

4.1.1 Primary products

The primary products observed in the N₂/O₂ experiment are butyrolactone (C₄H₆O₂), succinaldehyde (C₄H₆O₂) and propyl formate (C₄H₈O₂), the latter two as the primary ring-opening products. Reactions are shown in 1a and 1b. Reaction 1a shows following steps: 1) Hydrogen abstraction leads to formation of radical and HCl 2) Oxygen molecule (O₂) binds to radical position 3) Peroxy species (RO₂), where R represents an alkyl group or H only, abstracts an oxygen atom to form RO and O₂ 4.1) Hydrogen abstraction leads to the formation of butyrolactone 4.2) Ring-opening of radical 4.2.1) Decomposition of radical leads to formation of succinaldehyde. Reaction 1b shows the following steps: 1) Analogy to Reaction 1a (steps 1-3) 2) Ring-opening of radical 3) H binds to radical to form propyl formate. The reaction mechanism leading to the formation of the products in Reaction 1a and 1b, respectively, is consistent with the calculations made in the theoretical study, which shows that the barriers for hydrogen abstraction from the ring is lower close to the heterocyclic oxygen atom [9]. Step 4.1 and 4.2 are competing reaction ways which is shown in a similar study for the gas-phase reaction of OH with cyclohexane [23]. Cyclohexane (C₆H₁₂) consists of six carbon atoms in a ring structure and the results in the study apply for all cyclic compositions, i.e. THF and radicals of THF are included. Butyrolactone and propyl formate are identified by comparing their reference spectra [18] with the product spectra and the later also by identification of absorbance in regions characteristic for the functional group of esters, see Table 1. Figure 13 shows the reference spectra together with the product spectrum and Figure 14 shows a close up inspection on the ester absorption regions. Reference spectrum for succinaldehyde is calculated with Gaussian 09 [20] and is shown in Figure 15.



Reaction 1a. THF reacts in several steps to form butyrolactone resp. succinaldehyde.



Reaction 1b. THF ring-opens to form propyl formate.

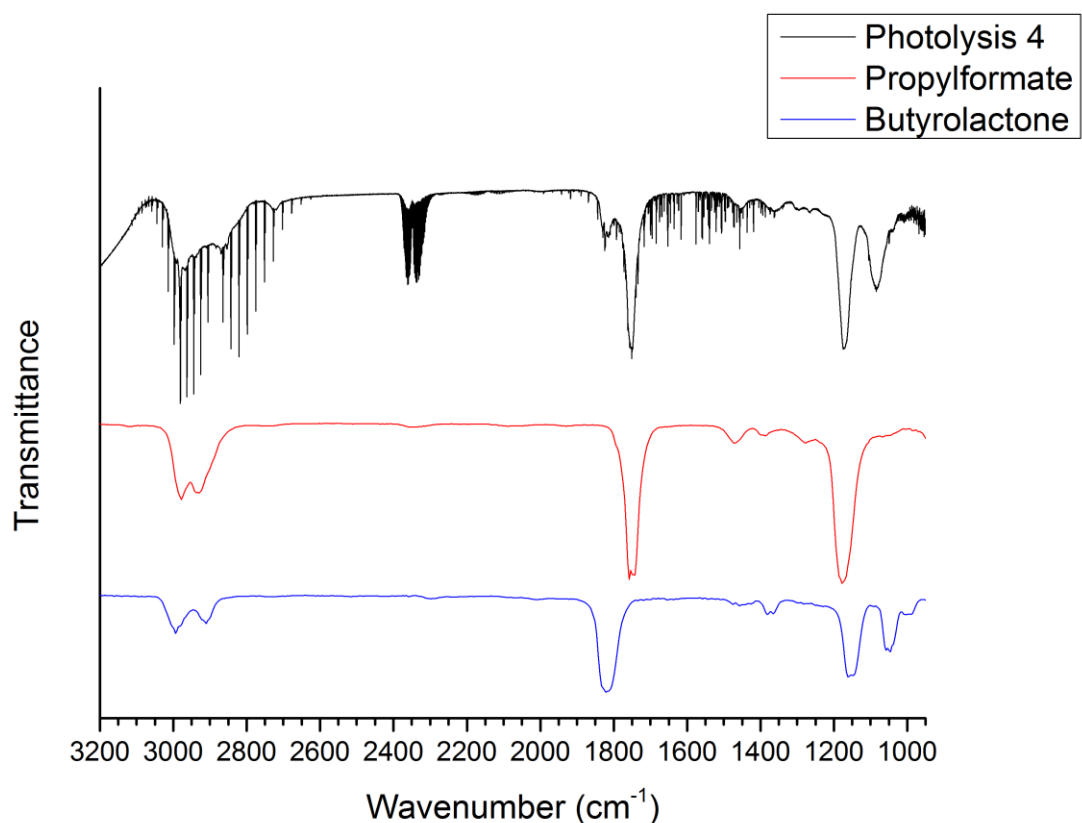


Figure 13. Product spectrum of photolysis 4 is shown together with reference spectra of propylformate (red line) and butyrolactone (blue line) [18]. The spectra are offset vertically.

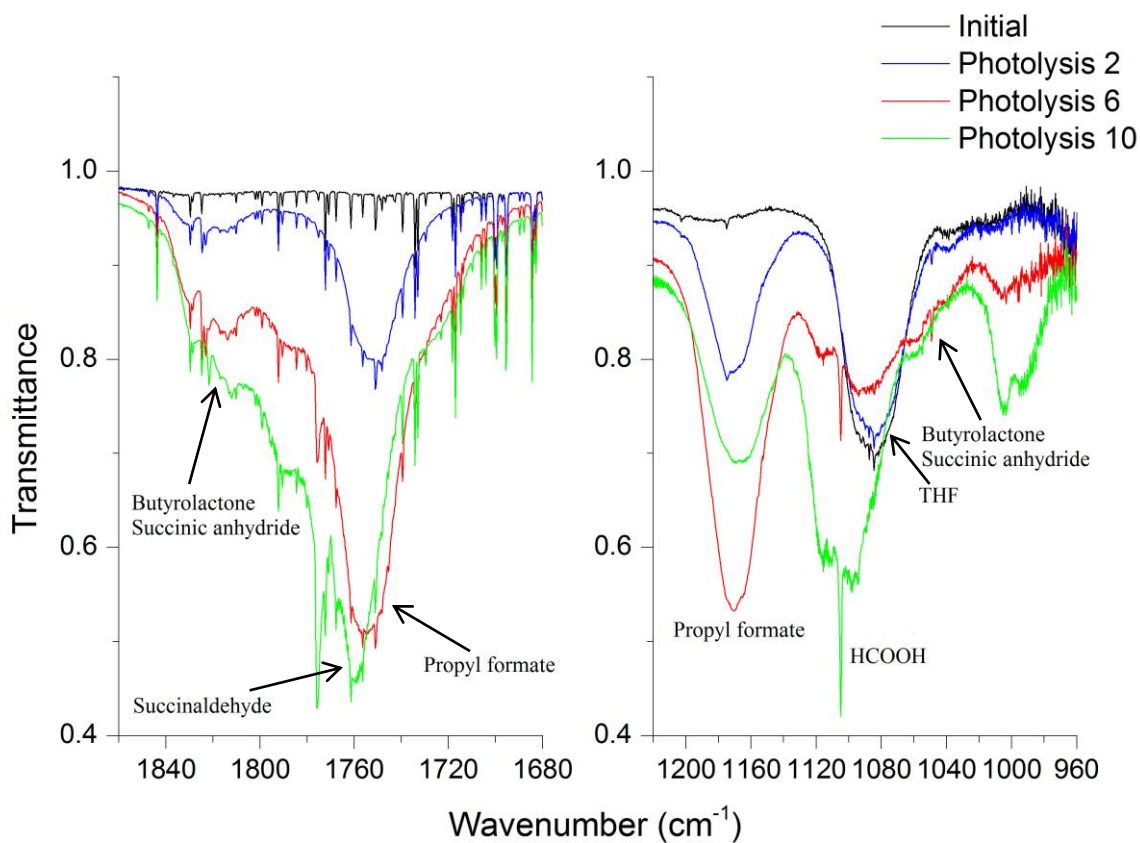
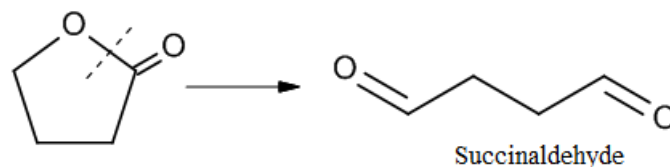


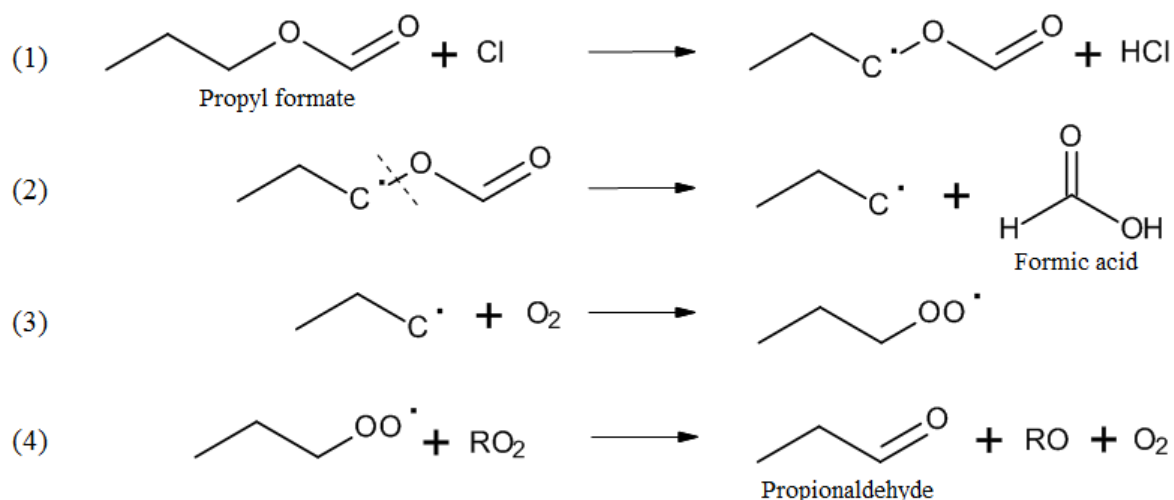
Figure 14. The initial spectrum and product spectrum of photolysis 2, 6 resp. 10 are shown in two different regions. Peaks corresponding to identified products are marked in the figure.

4.1.2 Secondary products

The secondary products observed are succinaldehyde ($C_4H_6O_2$), formic acid ($HCOOH$) and propionaldehyde (CH_3CH_2CHO). Succinaldehyde is the ring-opening product from butyrolactone while formic acid and propionaldehyde are products formed from propyl formate. Reactions are shown in 2a and 2b. Reaction 2a shows ring-opening of butyrolactone and Reaction 2b shows the following steps: 1) Hydrogen abstraction close to the oxygen 2) Radical decomposition into propyl radical and $HCOOH$ 3) O_2 binds to propyl radical 4) Hydrogen- and oxygen abstraction leads to formation of propionaldehyde. Studies have shown that thermal degradation of propyl formate decomposes into propene (C_3H_6) and formic acid, but since propene is not seen in this product study it is believed that in the conditions of this experiment, only the propyl radical is formed in step 1 [24]. Identification of succinaldehyde is made by comparing its calculated spectrum with the product spectra. Even though the calculated spectrum has low resolution, succinaldehyde is probable present in the product spectra due to its significant peak seen around 1750 cm^{-1} in the calculated spectrum and at 1760 cm^{-1} in the product spectra (photolysis 10), shown in Figure 15 and 14, respectively. Reference spectrum for propionaldehyde is taken from EUROCHAMP [19] and comparison with the product spectra makes propionaldehyde to a probable product as well, see Figure 16. The presence of formic acid is verified since its characteristic peaks are identified in the product spectra and its reference spectrum is available in high resolution. The formation of formic acid from propyl formate is likely since the concentration of propyl formate is starting to decrease as the concentration of formic acid is starting to increase, which is seen in Figure 14.



Reaction 2a. Butyrolactone ring-opens to form succinaldehyde.



Reaction 2b. Propyl formate reacts to form formic acid and propionaldehyde.

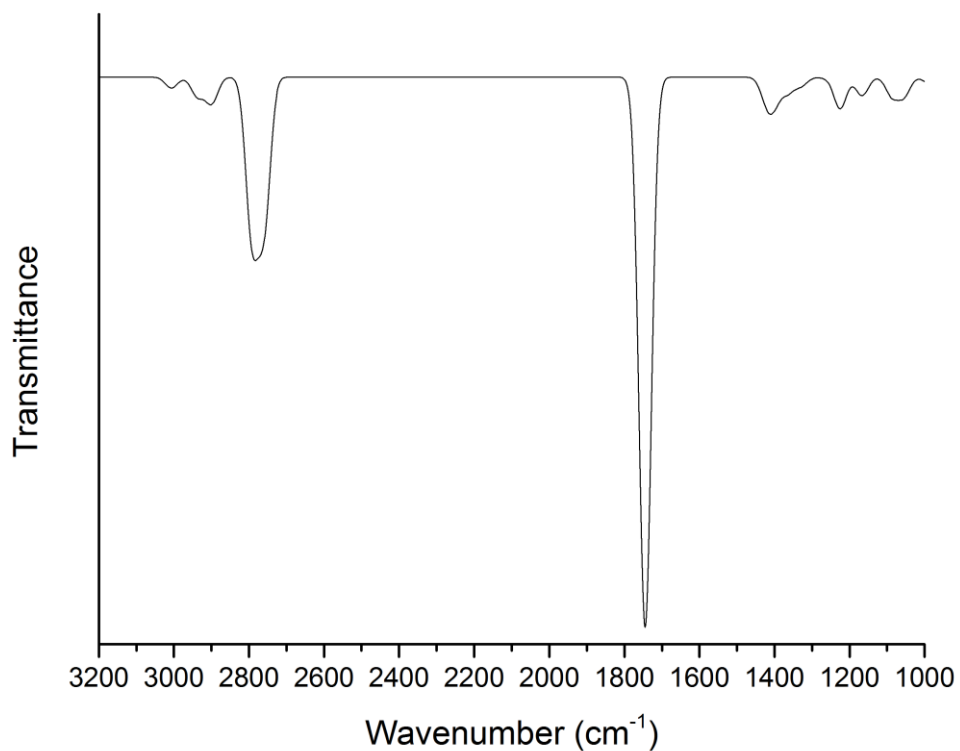


Figure 15. Calculated spectrum of succinaldehyde [20].

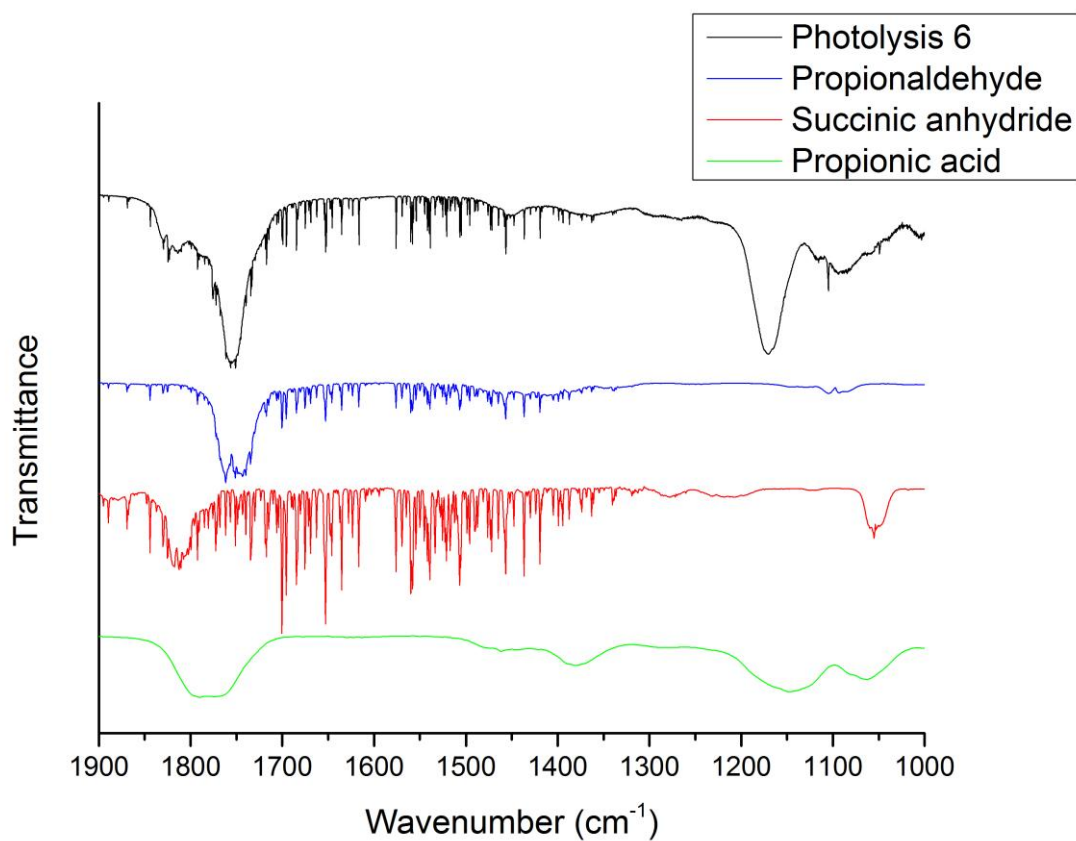
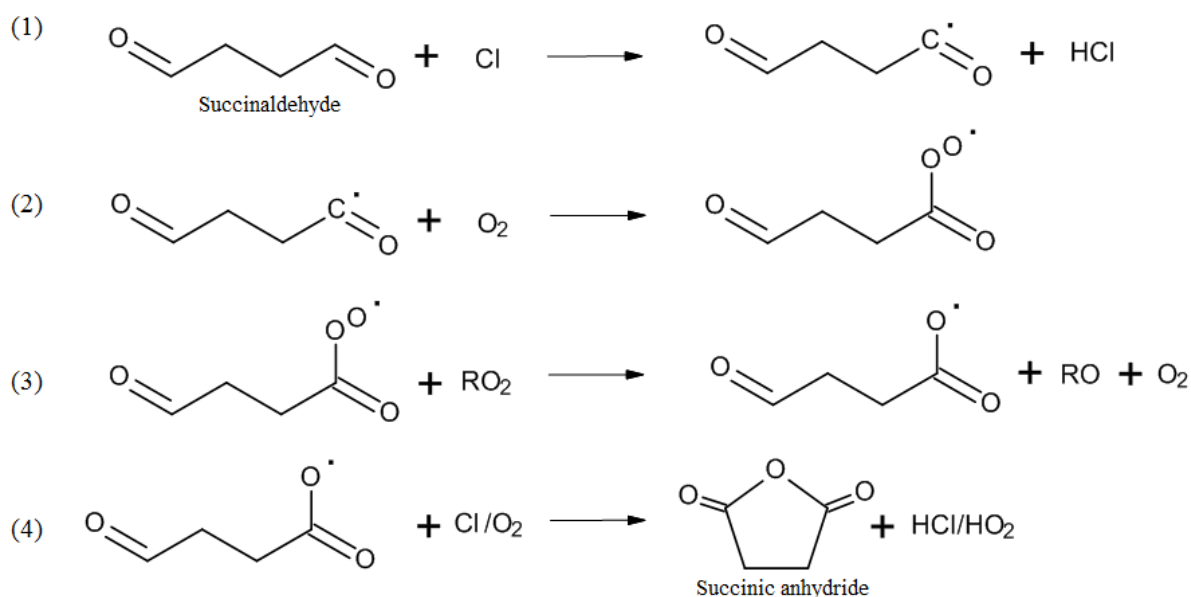


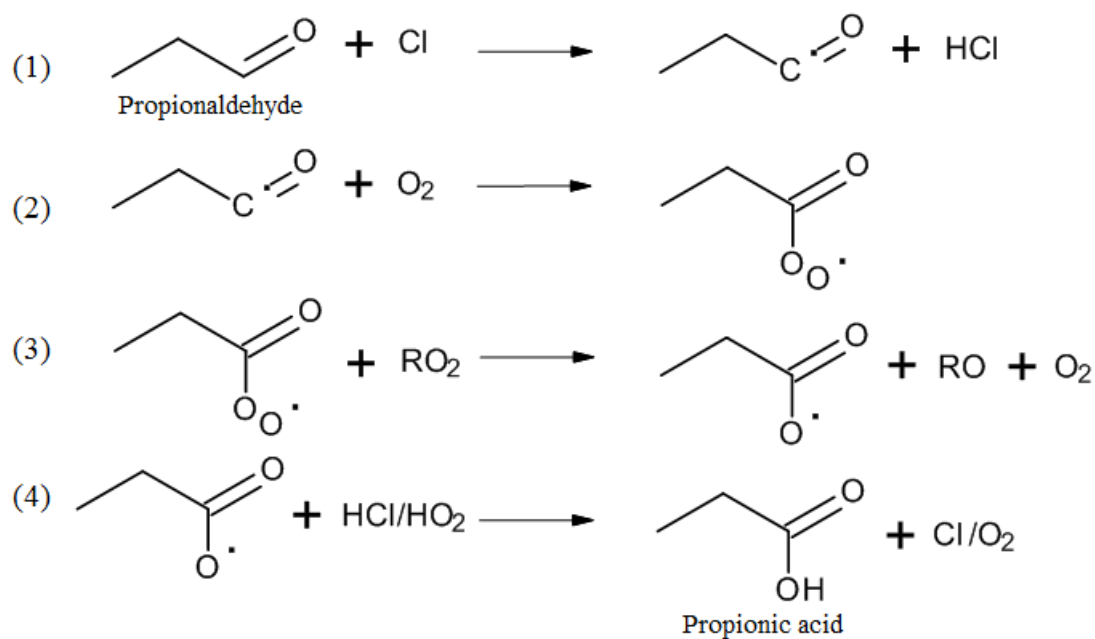
Figure 16. Product spectrum of photolysis 6 is shown together with reference spectra for propionaldehyde (blue line), succinic anhydride (red line) [19] and propionic acid (green line) [18]. The spectra are offset vertically.

4.1.3 Tertiary and later products

The tertiary products observed are succinic anhydride ($C_4H_4O_3$) and propionic acid (CH_3CH_2COOH), formed from succinaldehyde and propionaldehyde, respectively. Reactions are shown in 3a and 3b. Reaction 3a shows the following steps: 1-3) Analogy to Reaction 1a (steps 1-3) 4) Hydrogen abstraction leads to formation of succinic anhydride. Reaction 3b shows following step: 1-3) Analogy to Reaction 1a (steps 1-3) 4) Addition of hydrogen to radical leads to formation of propionic acid. Identification of succinic anhydride is made by comparing its reference spectrum taken from EUROCHAMP [19] with the product spectra, see Figure 16. Its presence, which is considered to be likely, indicates that the ring-structure is reshaped. Identification of propionic acid is made by comparing its reference spectrum taken from NIST [18] with the product spectra, see Figure 16. Even though the resolution is low of the reference spectrum, the formation of propionic acid from propionaldehyde is likely since it is in agreement with earlier studies [25].



Reaction 3a. Succinaldehyde reacts in several steps to form succinic anhydride.



Reaction 3b. Propionaldehyde reacts in several steps to form propionic acid.

A small amount of formaldehyde (H₂CO) is identified with its peak in concentration at photolysis 6-8. The entire reference spectrum of formaldehyde is shown in Figure 8 (lower panel) and the part of the spectrum used for identification is shown in Figure 17.

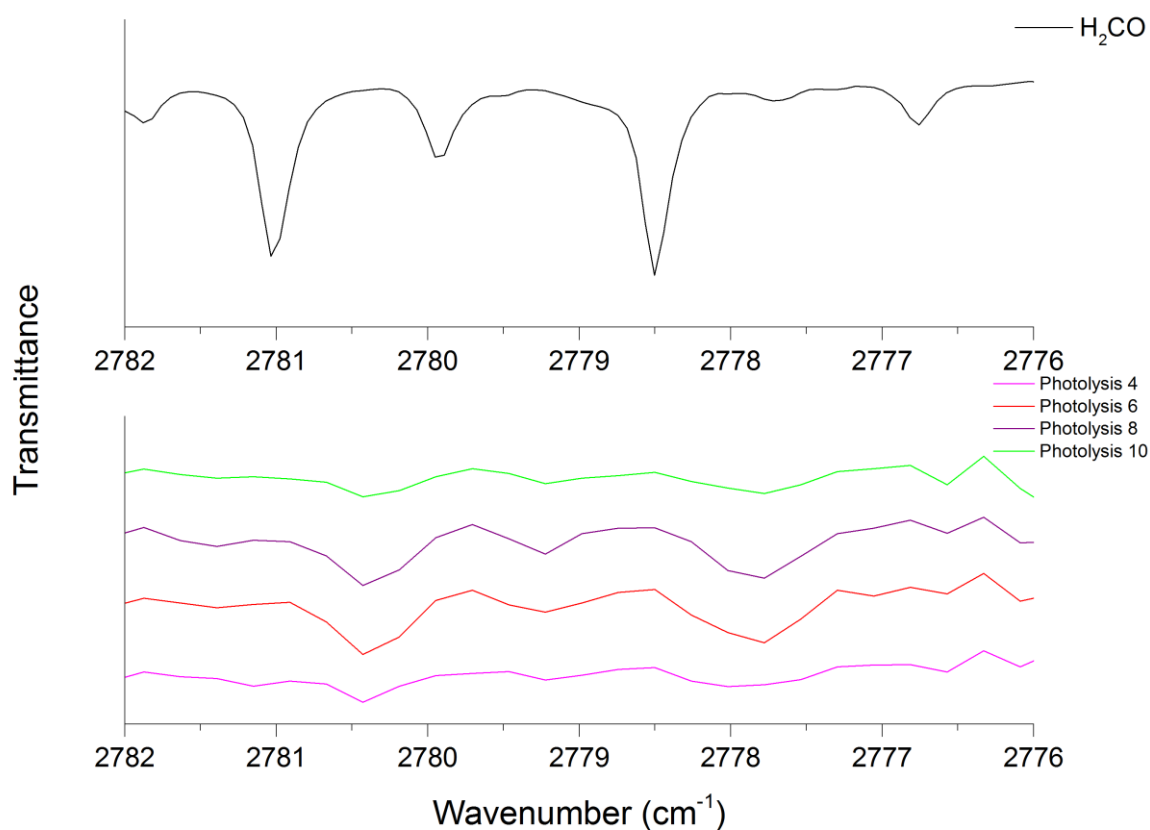


Figure 17. Upper panel: Reference spectrum of formaldehyde (H₂CO). Lower panel: Product spectra of photolysis 4, 6, 8 resp. 10. The spectra are offset vertically.

HCl is formed continuously during the experiment which is identified as the characteristic structure in the region $3050\text{-}2700\text{ cm}^{-1}$, shown in Figure 10 (upper panel). The formation of HCl is probably a result of the hydrogen abstraction as a common mechanism in the reaction series. CO and CO_2 are also formed continuously during the experiment, CO as a precursor to CO_2 . The stable character of CO_2 makes it the last step of the reaction series. A fitting of HCl, THF and CO is made with MALT, the first two fitted simultaneously, and the change in concentration with photolysis time of HCl and CO, respectively, is plotted against THF and presented in Figure 18.

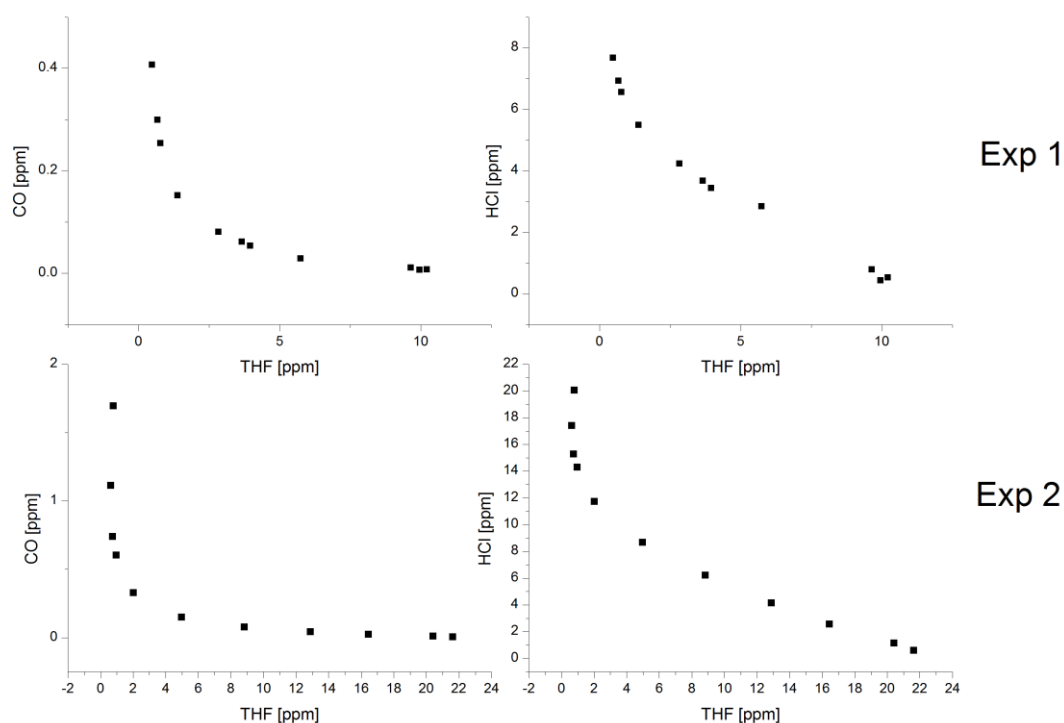


Figure 18. For N_2/O_2 photolysis series; the change of concentration for CO and HCl, respectively is plotted against THF. Upper panel: Experiment 1. Lower panel: Experiment 2.

In Figure 18, the concentration of THF is taken as a parameter of the experiment progression. The change of concentration for HCl can be divided into two regimes; one for the first six photolysis steps and one for the last ones. There is production of HCl from the start but the largest production occurs in the late experiment. The concentration of CO shows an almost negligible increase for the first six photolysis steps while for the last ones it increases significantly. Hence, the production of CO is a late step in the reaction mechanism and it is primarily produced in degradation of smaller molecules.

The reaction mechanisms leading to formation of the identified smaller molecules, i.e. HCOOH , H_2CO , HCl, CO and CO_2 are not completely determined. Thermal decomposition studies of succinic anhydride have been made showing that it decompose into C_2H_4 , CO and CO_2 [26]. The infrared absorption of C_2H_4 is primarily seen as fine structure at $\sim 3100\text{ cm}^{-1}$ and $\sim 950\text{ cm}^{-1}$, i.e. where the spectrometer used in this experiment loses signal. Hence, the

presence of C_2H_4 is possible but not verified and the consistency with the above mentioned study is undetermined.

Finally, there are probably still unidentified products in the spectra; for example, it is unclear what molecule the peak at 1000 cm^{-1} (Figure 14) corresponds to.

4.2 N_2 experiment

The product analysis for the Cl-initiated oxidation of THF in N_2 is, despite the fewer reactants, much more speculative. There are several hypotheses: The reaction mechanism in N_2 is believed to be similar to the mechanism in N_2/O_2 , but with the absence of oxygen as a major difference. As was shown in the results from the N_2/O_2 experiment, the oxygen and its derivatives show high reactivity towards both THF and products during the degradation mechanism. Without oxygen there is a hypothesis that Cl-atoms, which also tend to show high reactivity towards hydrocarbons would be the major oxidizer, i.e. chlorine-containing products are expected. The absence of experimental spectra of potential chlorinated products is the major reason for the speculative progression in the product study in N_2 . The hypothetical reaction mechanism is based on the mechanism for N_2/O_2 and analysis of calculated spectra [20].

Chlorination in different positions of a molecule will affect the infrared absorption regions, usually by shifting the peaks towards higher frequencies. Less absorption in the 3000 cm^{-1} region, which is observed in the product spectra, might be due to either lack of long alkane chains or chlorinated ones. An example of the effect of chlorination is shown in Figure 19. As seen in the upper panel of the figure, replacing the hydroxyl group in $HCOOH$ with a Cl atom to get $HCOCl$, the peak in the carbonyl region will strengthen and the other peaks will weaken. The peaks at $\sim 2900\text{ cm}^{-1}$ and $\sim 1200\text{ cm}^{-1}$ are observed to shift towards higher frequencies for $HCOCl$ compared to $HCOOH$. In the lower panel the effect of chlorination in different positions is observed. Chlorination close to the double-bonded oxygen, which is shown to the right, is seen to strengthen the peak in the carbonyl region and also shift it towards higher frequencies. The same reasoning applies for the peaks at $\sim 3000\text{ cm}^{-1}$.

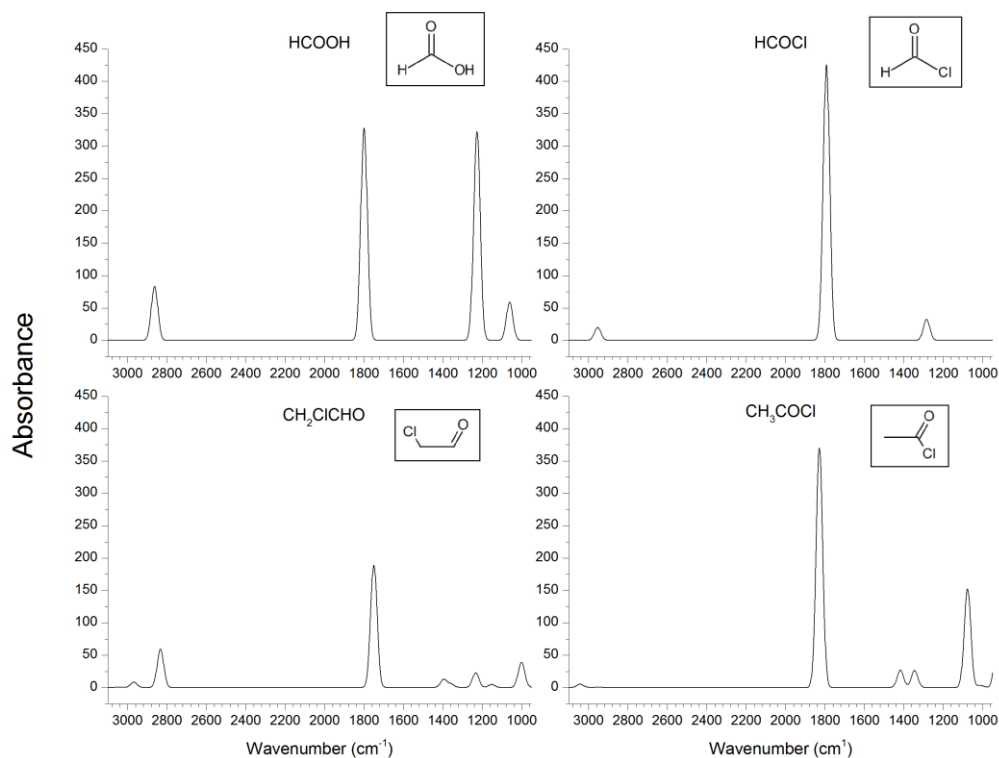
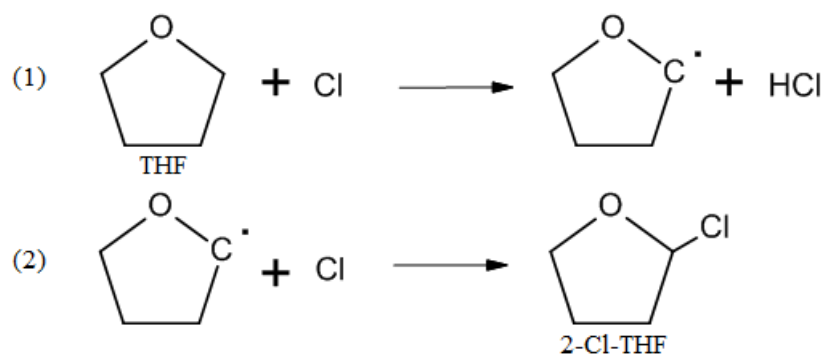
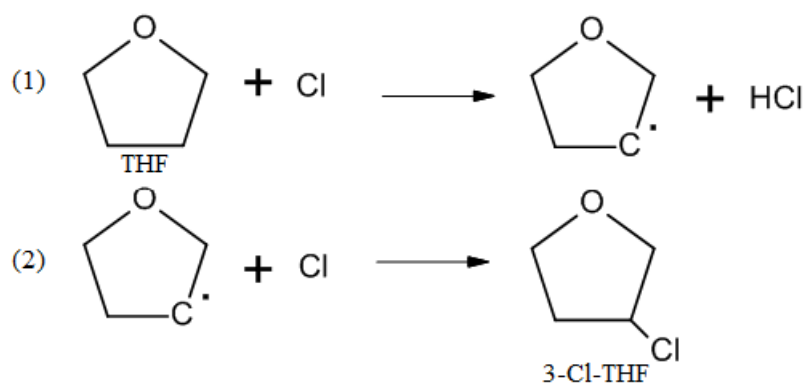


Figure 19. Calculated spectra of HCOOH, HCOCl, CH₂ClCHO and CH₃COCl, respectively [20] and the corresponding molecular structure.

In same manner as for N₂/O₂, the first step in the reaction chain is hydrogen abstraction from the ring, most probably close to the heterocyclic oxygen atom. The absence of reactive oxygen makes it more probable that Cl atoms add to the radical position. The two most probable reactions are shown in 4a and 4b. Reaction 4a shows the following steps: 1) Hydrogen abstraction leads to formation of radical and HCl 2) Cl atom binds to radical position. Reaction 4b (step 1-2) is analogous to Reaction 4a (step 1-2). Calculated spectra for THF and chlorinated compounds of THF are shown in Figure 20 together with the initial experimental spectrum and the second spectrum in the photolysis series. Only the absorption regions for the compounds are shown. When analysing the calculated spectra, primarily the relative strength and position of the peaks are of interest and less the actual position of the peak since they can involve a large shift. For a clearer figure visualisation, the calculated spectrum of THF has been matched to the initial experimental spectrum, which only consists of THF. Hence, the shift in the *x*-direction needed for matching the calculated THF with the “experimental THF” also applies for the other calculated spectra to maintain the relative positions.



Reaction 4a. THF reacts to form 2-Cl-THF.



Reaction 4b. THF reacts to form 3-Cl-THF.

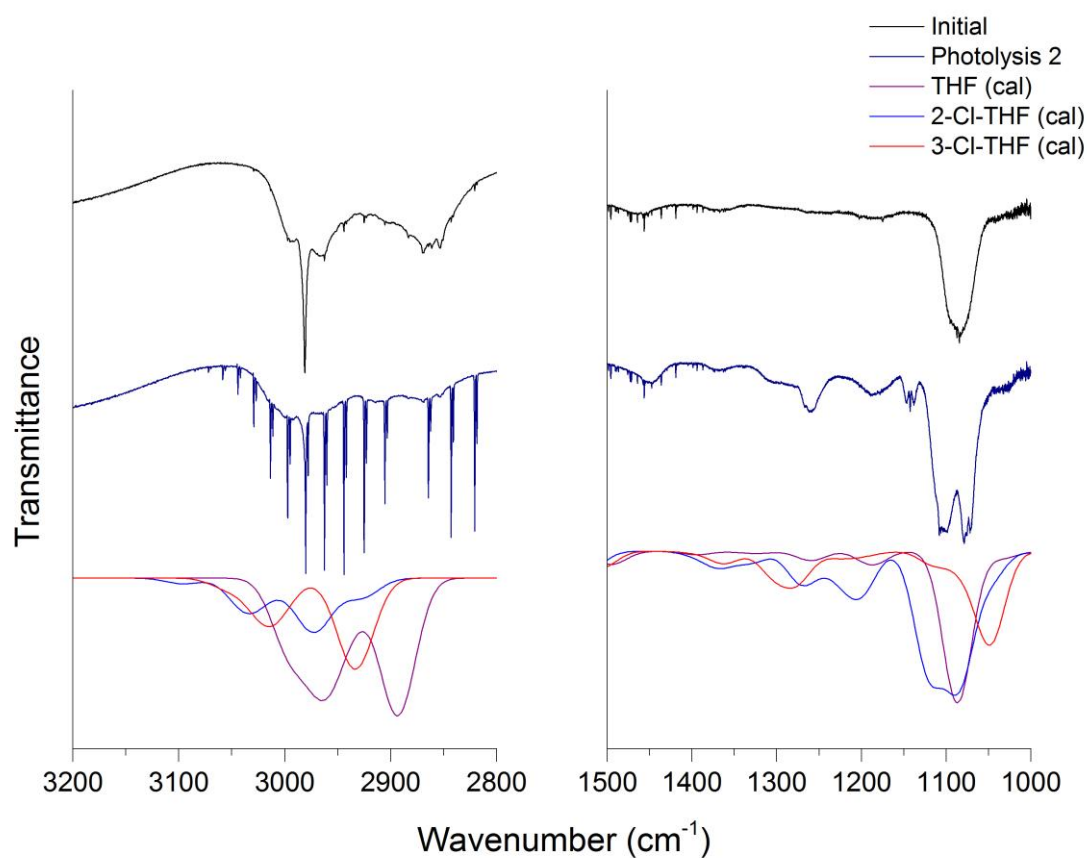
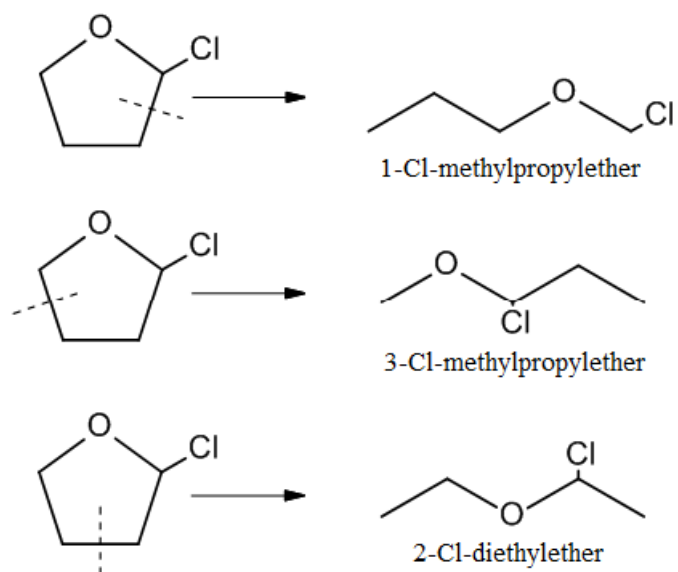


Figure 20. The initial spectrum and the product spectrum of photolysis 2 are shown together with calculated reference spectra of THF, 2-Cl-THF and 3-Cl-THF [20]. The spectra are offset vertically.

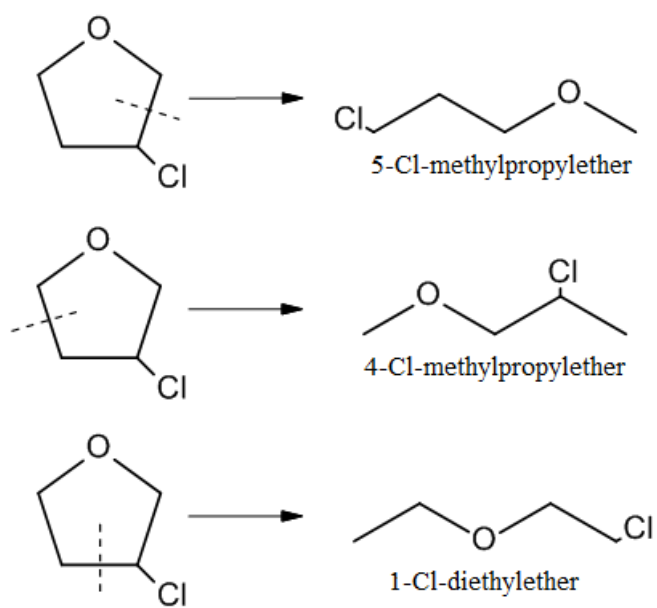
The difficulty in the type of analysis when the reference spectra do not show any detailed structures is primarily the overlaps. Molecules absorbing at partly the same frequencies will create a unique peak when they sum up, i.e. are present in the same spectrum. This reasoning applies also for the peaks corresponding to THF which decrease, but remain until the last photolysis steps in the experimental spectra.

However, analysis of Figure 20 motivates both 2-Cl-THF and 3-Cl-THF as potential products. To the right in the figure, showing the lower frequency region, following observations can be made: the peak corresponding to THF at 1100 cm^{-1} has not decreased at photolysis 2, rather it has increased which motivates the formation of other products in the region, the peak at 1040 cm^{-1} corresponding to 3-Cl-THF can be seen as a weak peak building up in photolysis 2 and it also supports the broadening of the 1100 cm^{-1} peak, 3-Cl-THF also builds up another weak peak at 1300 cm^{-1} . Slightly to the right, at about 1260 cm^{-1} , there is an overlap for 3-Cl-THF and 2-Cl-THF which probable accounts for the stronger peak seen at those frequencies in photolysis 2. The peak at 1200 cm^{-1} in the spectrum of 2-Cl-THF is probably seen in photolysis 2 at 1190 cm^{-1} , i.e. slightly shifted. 2-Cl-THF is also a product candidate due to its strong and broad peak at 1100 cm^{-1} , which accounts for the strengthening and broadening of the peak in that region. To the left in the figure, showing the higher frequency range there are also several observations made. By comparing the initial spectrum with the one from photolysis 2 something is seen building up in the region between the two strong peaks corresponding to THF. That can probably be 2-Cl-THF which has a relatively strong peak at 2940 cm^{-1} . It is also observed that the left peak of THF seems broader in photolysis 2, especially to the left (at 3025 cm^{-1}). This is probably due to the overlap of 2-Cl-THF and 3-Cl-THF seen at those frequencies. Also, the left peak does not decrease as fast as the right peak which gives indications of absorption by products in that region, which 2-Cl-THF actually shows.

Applying the ring-opening mechanism in N_2 motivates the formation of ethers. Reaction 5a and 5b show ethers that can possibly form from 2-Cl-THF and 3-Cl-THF by different ring-opening mechanisms. Identification of relatively strong absorption in the $1150\text{-}1070\text{ cm}^{-1}$ region, characteristic for the functional group of ethers supports the proposed mechanism, see Figure 21.



Reaction 5a. Ethers that can possibly form when 2-Cl-THF ring-opens.



Reaction 5b. Ethers that can possibly form when 3-Cl-THF ring-opens.

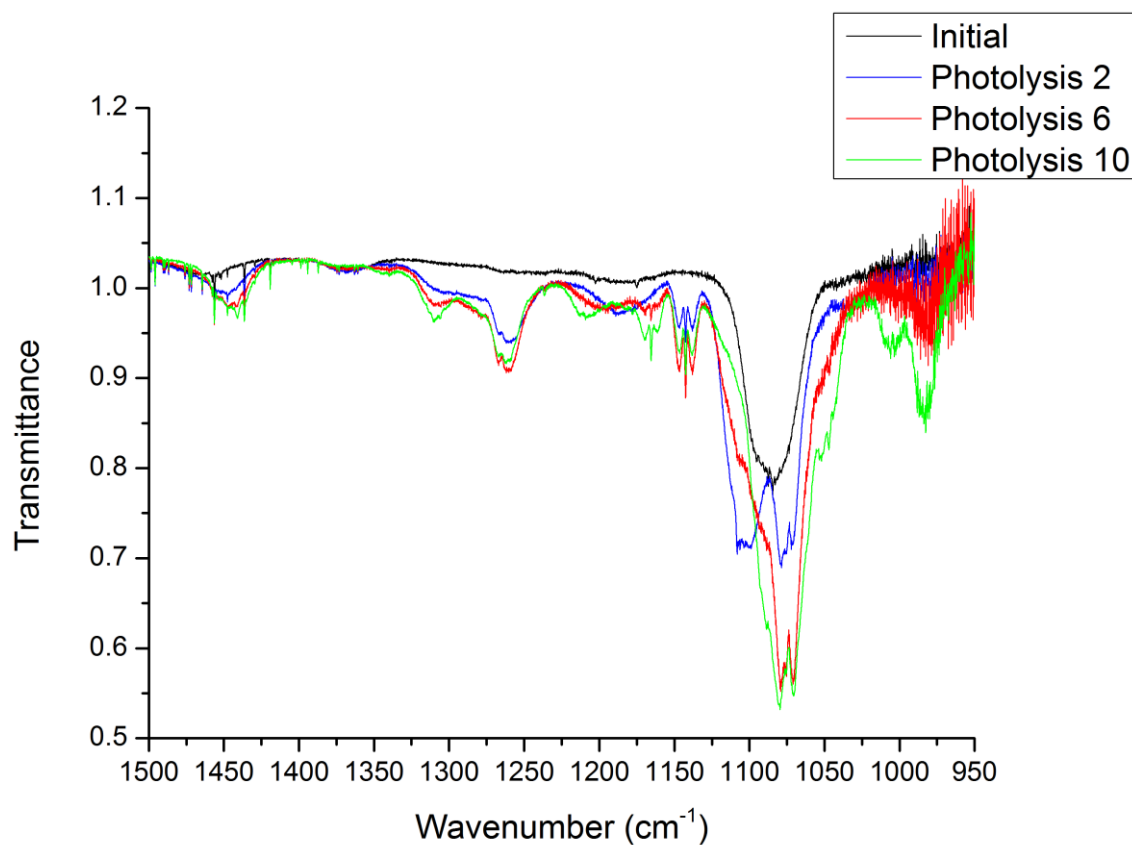


Figure 21. The initial spectrum and the product spectra of photolysis 2, 6 resp. 10 are shown in the fingerprint region.

Figure 22 shows the calculated spectra for the chlorinated ethers proposed in reaction 5a together with the initial experimental spectrum and several spectra from the photolysis series. The calculated spectrum of THF is again used as reference to enhance the visualisation.

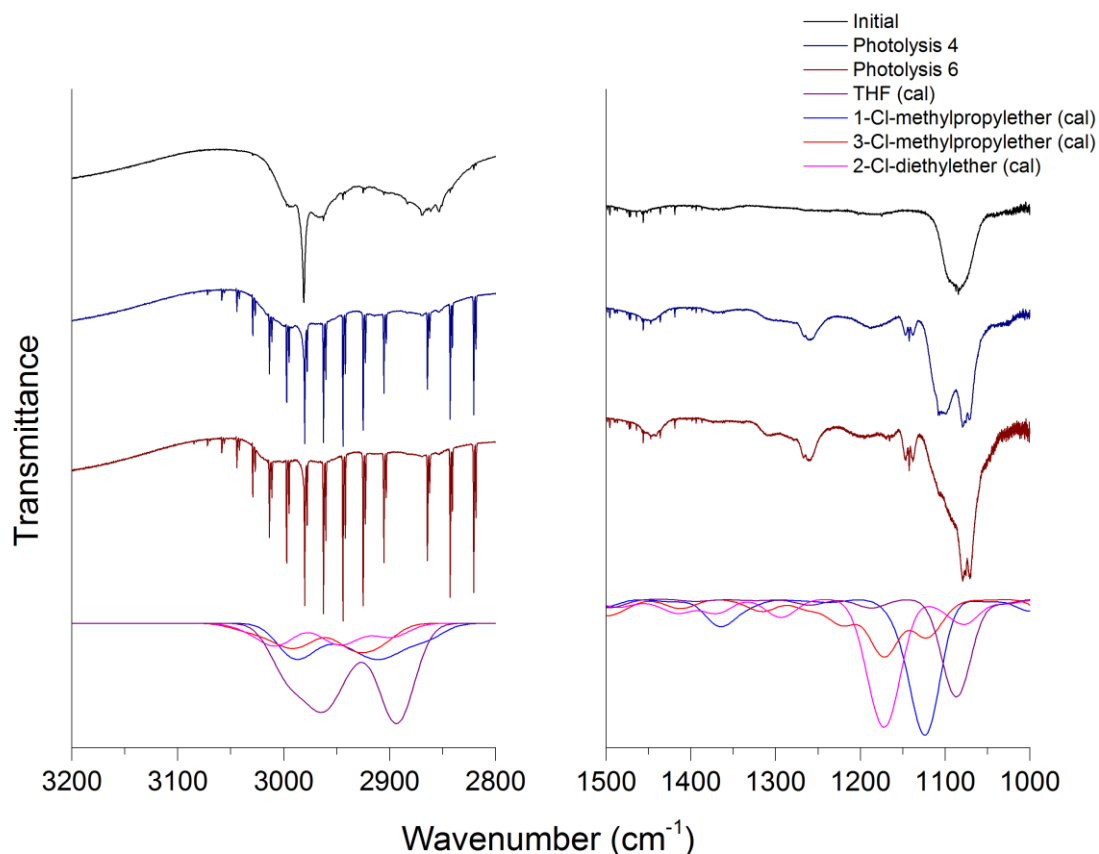


Figure 22. The initial spectrum and the product spectrum of photolysis 4 resp. 6 are shown together with calculated reference spectra of THF, 1-Cl-methylpropylether, 3-Cl-methylpropylether and 2-Cl-diethylether [20]. The spectra are offset vertically.

It is difficult to determine the probability of having the ethers showed in Figure 22 as products in the experimental spectra. Most probable is the 1-Cl-methylpropylether, which builds up a peak to the left of THF in the spectra, i.e. at a slighter higher frequency. But none of the proposed ethers can explain the strong peak at 1075 cm^{-1} building up continuous during the experiment. The detailed structure seen in the fingerprint region from 1125 cm^{-1} to 1500 cm^{-1} (see Figure 21) might be due to chlorinated ethers since chlorination tends to give fine-structured peaks even for larger molecules. If that is the case, even 3-Cl-methylpropylether is a potential product. However, fine-structured peaks are most probably indications of smaller molecules. Spectra, both experimental and calculated, of alkanes, alkenes and alcohols up to three carbon atoms in the molecule have been studied and also chlorinated such ones but none of the molecules have been identified. However, there is a chance that several of them are products in small amounts but are not seen due to overlaps.

There are indications of carbonyl groups in N_2 but the peaks are very weak, only a small amount of these molecules are present. Due to the reaction mechanism in N_2/O_2 it is eligible to believe that there are acids formed also in N_2 . The relatively high frequency absorption in the carbonyl region motivates the belief of acid chlorides, see Table 1. Calculated spectra of several acid chlorides are shown in Figure 19. Figure 23 shows the carbonyl region for N_2 .

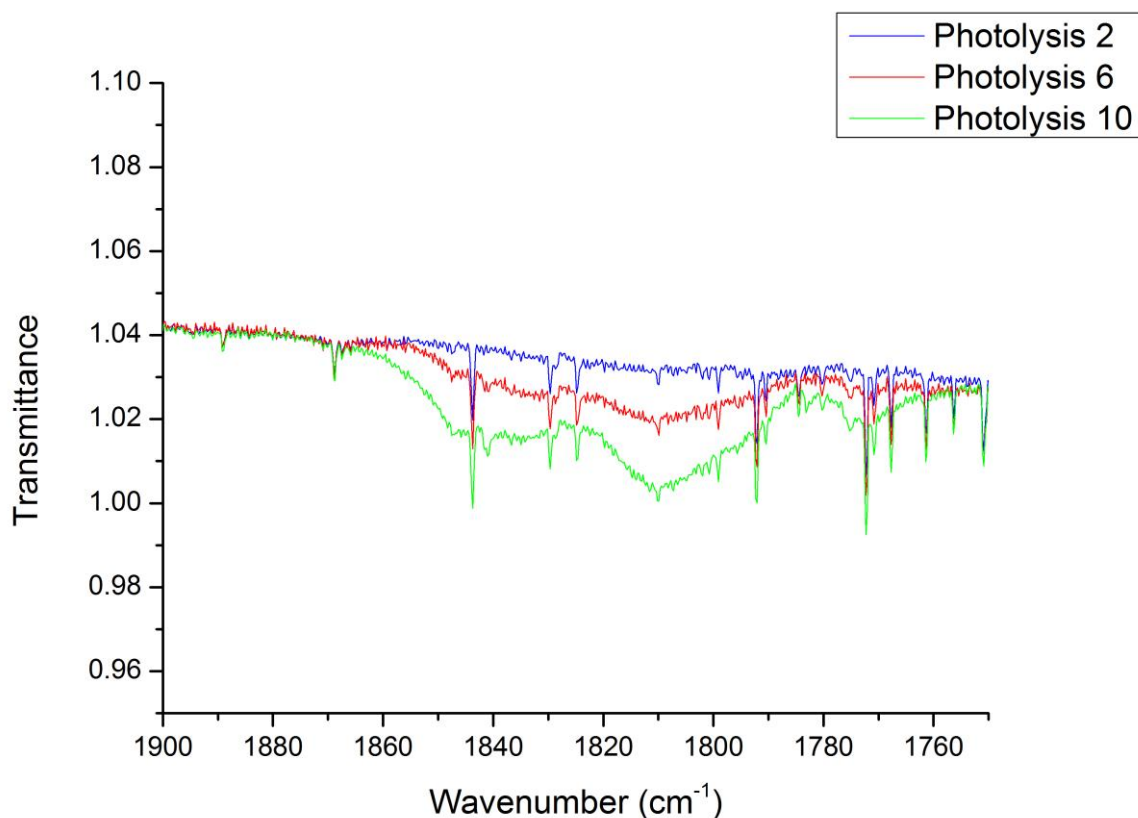


Figure 23. The product spectra of photolysis 2, 6 resp. 10 are shown in the carbonyl region.

The absorption regions in Figure 23 at 1775 cm^{-1} , 1815 cm^{-1} and 1845 cm^{-1} can possibly correspond to CH_2ClCHO , HCOCl and CH_3COCl , respectively, for which calculated spectra are shown in Figure 19.

HCl is formed in approximately the same amount as in the N_2/O_2 experiment and probably for the same reason, namely hydrogen abstraction. CO and CO_2 are also formed continuously during the experiment but in much smaller amounts than for the N_2/O_2 experiment. In the same manner as for the N_2/O_2 experiment, a fitting of HCl, THF and CO is made with MALT and the change in concentration with photolysis time of HCl and CO, respectively is plotted against THF and is presented in Figure 24.

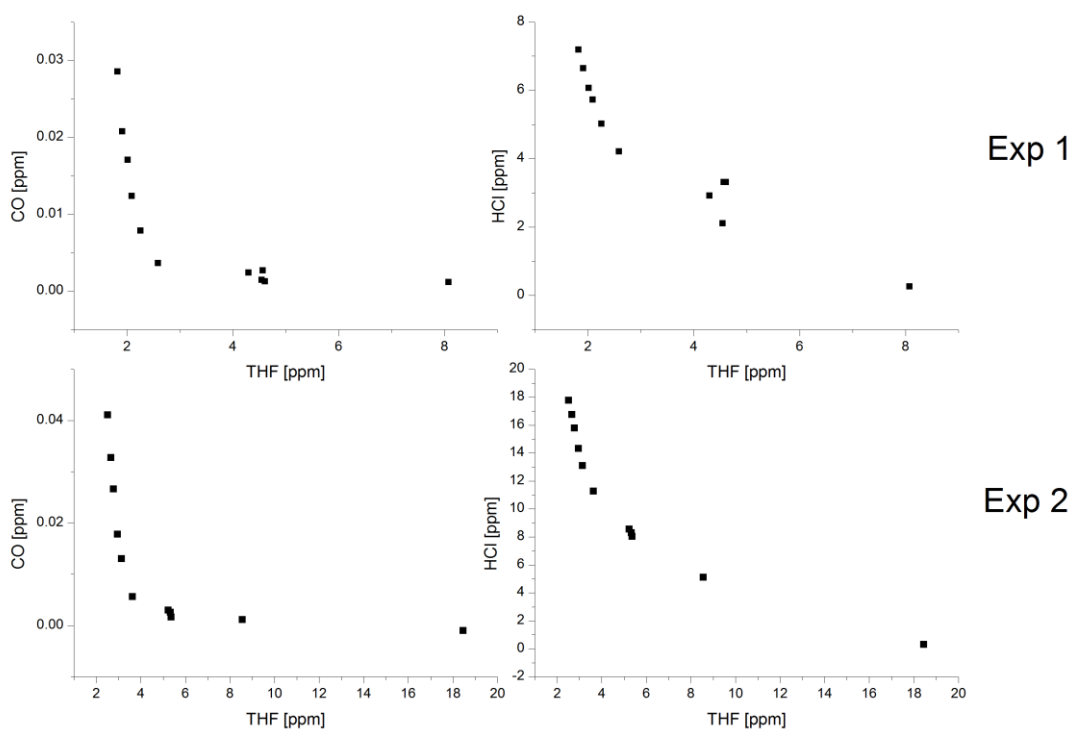


Figure 24. For N_2 photolysis series; the change of concentration for CO and HCl are plotted against THF. Upper panel: Experiment 1. Lower panel: Experiment 2.

The correlations show the same trend as for the N_2/O_2 experiment with the largest increase of HCl and CO at the end of the experiment.

To summarize the product study in N_2 , all the THF has reacted in the end of the experiment, i.e. only products are present in the last spectrum. However, these products might be predominantly larger molecules, such as chlorinated ethers due to the unsuccessful attempts to identify smaller molecules. If that is the case, the reaction in N_2 is slower than in N_2/O_2 , which perhaps is due to the fewer reactants.

5. Conclusion

The majority of the products in the N₂/O₂ experiment have been determined but there are still some peaks in the photolysis series corresponding to unknown products. A complete product distribution is necessary to be able to determine the reaction mechanism.

None of the products in the N₂ experiment are verified but there are indications of chlorinated molecules. For further identification of products in the N₂ photolysis series, high-resolution reference spectra would be advantageous.

In both experimental spectra, there are many molecules overlapping which make the product verification difficult. Many of the proposed products absorb at frequencies outside the region of the experimental spectra and examination of these would give more information about the molecules. Hence, an advantage would be to have signal from a broader infrared region, which requires other spectrometer equipment. Additional information would be obtained if other spectroscopy methods were used, such as mass spectroscopy and nuclear magnetic resonance spectroscopy.

An advantage of the reaction mechanism would be to know the concentrations of each product and the change of concentration with photolysis time. This information can be obtained by analysis with MALT but require high-resolution reference spectra for the fitting procedure.

Conclusions that can be drawn are that all THF have reacted in the end of the experiment for both experiments, thus react fast with Cl-atoms. This knowledge is of great importance especially in marine regions, industrial polluted- and urban areas where the Cl concentration is usually high. Noteworthy is also the fact that a completed reaction would only consist of CO₂ since that is considered to be the most stable molecule formed during the experiment. Since there are still other products than CO₂ in the last spectra of the experiments, the reactions are not completed.

Advantageous in order to investigate the environmental impact of THF would be to make a similar study of the OH-initiated oxidation of THF since the OH radical is one of the most important oxidizers around the world.

References

- [1] Solomon, S., Qin, D., Manning, M., Chen, Z., Marquis, M., Averyt, K. B., Tignor, M. and Miller, H. L. (eds.) (2007), IPCC, 2007: Summary for Policemakers: Climate change 2007: The Physical Science Basis. Contribution of Working Group I to the Fourth Assessment Report of the Intergovernmental Panel on Climate Change, *Cambridge University Press*, Cambridge, United Kingdom and New York, NY, USA
- [2] Demirbas, A. (2009), Biofuels – Securing the Planet’s Future Energy Needs, *Green Energy and Technology*, Springer-Verlag London Limited
- [3] Sims, R., Taylor, M., Saddler, J., Mabee, W. (2008), From 1st- To 2nd- Generation Biofuel Technologies – An overview of current industry and RD&D activities, *IEA Bioenergy*, OECD/IEA
- [4] Jacobson, M. Z. (2007), Effects of ethanol (E85) versus gasoline vehicles on cancer and mortality in the United States, *Environmental Science & Technology*, Vol. 41, No. 11, pp. 4150-4157
- [5] Moriarty, J., Sidebottom, H., Wenger, J., Mellouki, A. and Le Bras, G. (2003), Kinetic Studies on the Reactions of Hydroxyl Radicals with Cyclic Ethers and Aliphatic Diethers, *The Journal of Physical Chemistry A*, Vol. 107, No. 10, pp. 1499-1505
- [6] Alwe, H. D., Walawalkar, M., Sharma, A., Pushpa, K. K., Dhanya, S. and Naik, P. D. (2012), Rate Coefficients for the Gas-Phase Reactions of Chlorine Atoms with Cyclic Ethers at 298 K, *International Journal of Chemical Kinetics*, Wiley Periodicals, Inc.
- [7] Giri, B. R. and Roscoe, J. M. (2010), Kinetics of the Reactions of Cl Atoms with Several Ethers, *The Journal of Physical Chemistry A*, Vol. 114, No. 32, pp. 8369-8375
- [8] Young, C. J., Washenfelder, R. A., Edwards, P. M., Parrish, D. D., Gilman, J. B., Kuster, W. C., Mielke, L. H., Osthoff, H. D., Tsai, C., Pikelnaya, O., Stutz, J., Veres, P. R., Roberts, J. M., Griffith, S., Dusanter, S., Stevens, P. S., Flynn, J., Grossberg, N., Lefer, B., Holloway, J. S., Peischl, J., Ryerson, T. B., Atlas, E. L., Blake, D. R. and Brown, S. S. (2013), Evaluating evidence for Cl sources and oxidation chemistry in a coastal, urban environment, *Atmospheric Chemistry and Physics Discussions*, Vol. 13, pp. 13685-13720
- [9] Simmie, J. M. (2012), Kinetics and Thermochemistry of 2,5-Dimethyltetrahydrofuran and Related Oxolanes: Next Next-Generation Biofuels, *The Journal of Physical Chemistry A*, Vol. 116, No. 18, pp. 4528-4538
- [10] Bierbach, A., Barnes, I. and Becker, K. H. (1995), Product and kinetic study of the OH initiated gas-phase oxidation of furan, 2-methylfuran and furanaldehydes at ≈ 300 K, *Atmospheric Environment*, Vol. 29, No. 19, pp. 2651-2660
- [11] Villanueva, F., Barnes, I., Monedero, E., Salgado, S., Gómez, V. and Martin, P. (2007), Primary product distribution from the Cl-atom initiated atmospheric degradation of furan: Environmental implications, *Atmospheric Environment*, Vol. 41, pp. 8796-8810

- [12] Seinfeld, J. H. and Pandis, S. N. (2006), Atmospheric chemistry and physics – from air pollution to climate change, 2nd edition, *John Wiley & Sons Inc.*, Hoboken, New Jersey
- [13] Adams, J. W. and Cox, R. A. (2002), Halogen chemistry of the marine boundary layer, *Journal De Physique IV France*, 12, EDP Sciences, Les Ulis
- [14] Engel, T. (2013), Quantum Chemistry and Spectroscopy, 3rd edition, *Pearson Education, Inc.*, United States
- [15] Williams, D. H. and Fleming, I. (1995), Spectroscopic methods in organic chemistry, 5th edition, *McGraw-Hill Higher Education*, UK
- [16] Ausmeel, S. (2012), Furans – The potential atmospheric impact of a next-generation bio fuel, *Lund University*, Sweden
- [17] Nilsson, E. J. K., Eskebjerg, C. and Johnson, M. S. (2009), A photochemical reactor for studies of atmospheric chemistry, *Atmospheric Environment*, Vol. 43, pp. 3029-3033
- [18] Linstrom, P. J. and Mallard, W. G., Eds., NIST Chemistry WebBook, NIST Standard Reference Database Number 69, *National Institute of Standards and Technology*, Gaithersburg MD, 20899, (Online) Available: Internet <<http://webbook.nist.gov>> (retrieved June 7, 2013)
- [19] EUROCHAMP FTIR Spectral database, (Online) Available: Internet <<http://euphore.es/FTIRReferences2/index.php>> (Downloaded May 2013)
- [20] Frisch, M. J., Trucks, G. W., Schlegel, H. B., Scuseria, G. E., Robb, M. A., Cheeseman, J. R., Scalmani, G., Barone, V., Mennucci, B., Petersson, G. A., Nakatsuji, H., Caricato, M., Li, X., Hratchian, H. P., Izmaylov, A. F., Bloino, J., Zheng, G., Sonnenberg, J. L., Hada, M., Ehara, M., Toyota, K., Fukuda, R., Hasegawa, J., Ishida, M., Nakajima, T., Honda, Y., Kitao, O., Nakai, H., Vreven, T., Montgomery, Jr., J. A., Peralta, J. E., Ogliaro, F., Bearpark, M., Heyd, J. J., Brothers, E., Kudin, K. N., Staroverov, V. N., Kobayashi, R., Normand, J., Raghavachari, K., Rendell, A., Burant, J. C., Iyengar, S. S., Tomasi, J., Cossi, M., Rega, N., Millam, J. M., Klene, M., Knox, J. E., Cross, J. B., Bakken, V., Adamo, C., Jaramillo, J., Gomperts, R., Stratmann, R. E., Yazyev, O., Austin, A. J., Cammi, R., Pomelli, C., Ochterski, J. W., Martin, R. L., Morokuma, K., Zakrzewski, V. G., Voth, G. A., Salvador, P., Dannenberg, J. J., Dapprich, S., Daniels, A. D., Farkas, Ö., Foresman, J. B., Ortiz, J. V., Cioslowski, J. and Fox, D. J. (2009), Gaussian 09, Revision A.1, *Gaussian Inc.*, Wallingford CT
- [21] Griffith, D. W. T. (1996), Synthetic calibration and quantitative analysis of gas-phase FT-IR spectra, *Applied Spectroscopy*, Vol. 50, pp. 59-70

- [22] Rothman, L. S., Gordon, I. E., Barbe, A., Benner, D. C., Bernath, P. E., Birk, M., Boudon, V., Brown, L. R., Campargue, A., Champion, J. P., Chance, K., Coudert, L. H., Dana, V., Devi, V. M., Fally, S., Flaud, J. M., Gamache, R. R., Goldman, A., Jacquemart, D., Kleiner, I., Lacome, N., Lafferty, W. J., Mandin, J. Y., Massie, S. T., Mikhailenko, S. N., Miller, C. E., Moazzen-Ahmadi, N., Naumenko, O. V., Nikitin, A. V., Orphal, J., Perevalov, V. I., Perrin, A., Predoi-Cross, A., Rinsland, C. P., Rotger, M., Simeckova, M., Smith, M. A. H., Sung, K., Tashkun, S. A., Tennyson, J., Toth, R. A., Vandaele, A. C. and Vander Auwera, J. (2009), The HITRAN 2008 molecular spectroscopic database, *Journal of Quantitative Spectroscopy & Radiative Transfer*, Vol. 110, No. 9-10, pp. 533-572
- [23] Aschmann, S. M., Chew, A. A., Arey, J. and Atkinson, R. (1997), Products of the Gas-Phase Reaction of OH Radicals with Cyclohexane: Reactions of the Cyclohexoxy Radical, *The Journal of Physical Chemistry A*, Vol. 101, No. 43, pp. 8042-8048
- [24] Anderson, R. B., Rowley, H. H. (1943), Kinetics of the thermal decomposition of n-propyl and isopropyl formates, *The Journal of Physical Chemistry*, Vol. 52, pp. 454-463
- [25] Le Crâne, J-P., Villenave, E., Hurley, M. D., Wallington, T. J. and Ball, J. C. (2005), Atmospheric Chemistry of Propionaldehyde: Kinetics and Mechanisms of Reactions with OH Radicals and Cl Atoms, UV Spectrum, and Self-Reaction Kinetics of CH₃CH₂C(O)O₂ Radicals at 298 K, *The Journal of Physical Chemistry A*, Vol. 109, No. 51, pp. 11837-11850
- [26] Yamamoto, S. and Back, R. A. (1983), The thermal and photochemical decompositions of succinic anhydride and 2,3-dimethyl succinic anhydride in the gas phase, *Canadian Journal of Chemistry*, Vol. 61, No. 12, pp. 2790-2794